haematologica
Journal of the Ferrata Storti Foundation

Steroid-free combination of 5-azacytidine and venetoclax for the treatment of multiple myeloma

by Lyndsey Flanagan, Aisling Y. Coughlan, Nicola Cosgrove, Andrew Roe, Yu Wang, Stephanie Gilmore, Izabela Drozdz, Claire Comerford, Jeremy Ryan, Emma Minihane, Salma Parvin, Michael O'Dwyer, John Quinn, Philip Murphy, Simon Furney, Siobhan Glavey, and Tríona Ní Chonghaile.
Collaborative Groups: Leukemia Research Foundation (Triona Ni Chonghaile, Lyndsey Flanagan), Science Foundation Ireland (Triona Ni Chonghaile), Breakthrough Cancer Research (Lyndsey Flanagan).

Received: June 29, 2023.
Accepted: March 8, 2024.

Citation: Lyndsey Flanagan, Aisling Y. Coughlan, Nicola Cosgrove, Andrew Roe, Yu Wang, Stephanie Gilmore, Izabela Drozdz, Claire Comerford, Jeremy Ryan, Emma Minihane, Salma Parvin, Michael O'Dwyer, John Quinn, Philip Murphy, Simon Furney, Siobhan Glavey, and Tríona Ní Chonghaile. Collaborative Groups: Leukemia Research Foundation (Triona Ni Chonghaile, Lyndsey Flanagan), Science Foundation Ireland (Triona Ni Chonghaile), Breakthrough Cancer Research (Lyndsey Flanagan). Steroid-free combination of 5-azacytidine and venetoclax for the treatment of multiple myeloma. Haematologica. 2024 Mar 21. doi: 10.3324/haematol.2023.283771 [Epub ahead of print]

Steroid-free combination of 5-azacytidine and venetoclax for the treatment of multiple myeloma.

Lyndsey Flanagan[1], Aisling Coughlan[1], Nicola Cosgrove[1], Andrew Roe[1], Yu Wang[1], Stephanie Gilmore[1], Izabela Drozdz[2], Claire Comerford[2,3], Jeremy Ryan[4], Emma Minihane[4], Salma Parvin[4], Michael O'Dwyer[5], John Quinn[2,3], Philip Murphy[2,3], Simon Furney[1], Siobhan Glavey[2,3#], Tríona Ní Chonghaile [1*,#]

[1]Physiology and Medical Physics**,** Royal College of Surgeons in Ireland, 123 St. Stephen's Green, Dublin 2, Ireland.
[2] Department of Pathology, Royal College of Surgeons in Ireland
[3] Department of Haematology, Beaumont Hospital, Dublin, Ireland
[4] Department of Medical Oncology, Dana-Farber Cancer Institute, Boston, MA
[5] Department of Medicine/Haematology, University of Galway, Galway, Ireland

Keywords: Ven, BCL-2, Multiple Myeloma, epigenetics, 5-azacytidine
Running title: Inducing BCL-2 dependence in Multiple Myeloma

[#]Shared senior authorship, correspondence addressed to:

Tel:+353014028579
Email: tnichonghaile@rcsi.com

Competing interests:

TNC received research funding from AbbVie. JQ has the following disclosures Honoraria for Janssen and Takeda and Travel funding from Roche. MOD has no competing interest but has employment and equity in ONK Therapeutics.

Author contributions:

TNC and SG designed the study and co-wrote the paper. LF performed experiments, analyzed data and co-wrote the manuscript. AC, NC, AR, YW, SG, ID, CC, JR, EM, SG and SP performed experiments and analyzed data. MOD, JQ, PM and SF designed experiments and all authors read and edited the manuscript.

Data availability statement:

All data will be made freely available to any researcher wishing to use it for non-commercial purposes.

Acknowledgements:

The authors would like to thank the following funding agencies for their support: the Leukemia Research Foundation (LRF-RCSI-2020) and Science Foundation Ireland (19/FFP/6461) support TNC, Breakthrough Cancer Research (BCR-RCSI-2020) support LF.

Abstract

Multiple Myeloma (MM) is an incurable plasma cell malignancy, that despite an unprecedented increase in overall survival, lacks truly risk-adapted or targeted treatments. A proportion of patients with MM depend on BCL-2 for survival and recently the BCL-2 antagonist venetoclax has shown clinical efficacy and safety in t(11;14) and BCL-2 overexpressing MM. However, only a small proportion of MM patients rely on BCL-2 (~20%), there is a need to broaden the patient population outside of t(11;14) that can be treated with venetoclax. Therefore, we took an unbiased screening approach and screened epigenetic modifiers to enhance venetoclax sensitivity in two non-BCL-2 dependent MM cell lines. The demethylase inhibitor 5-azacytidine was one of the lead hits from the screen, and the enhanced cell killing of the combination was confirmed in additional MM cell lines. Using dynamic BH3 profiling and immunoprecipitations we identified the potential mechanism of synergy is due to increased NOXA expression, through the integrated stress response. Knockdown of *PMAIP1* or *PKR* partially rescues cell death of the venetoclax and 5-azacytidine combination treatment. The addition of a steroid to the combination treatment did not enhance the cell death and interestingly we found enhanced death of the immune cells with steroid addition, suggesting that a steroid-sparing regimen may be more beneficial in MM. Lastly, we show for the first time in primary MM patient samples, that 5-azacytidine enhances the response to venetoclax *ex-vivo*, across diverse anti-apoptotic dependencies (BCL-2 or MCL-1) and diverse cytogenetic backgrounds. Overall, our data identifies 5-azacytidine and venetoclax as an effective treatment combination and this could be a tolerable steroid-sparing regimen, particularly for elderly MM patients.

Key points:

- Epigenetic modifier screen identifies the steroid-free synergistic combination of 5-azacytidine and venetoclax, effective *ex-vivo* in Multiple Myeloma patient samples irrespective of cytogenetics
- 5-azacytidine induces the expression of NOXA through the integrated stress response, antagonising MCL-1 and sensitising cells to venetoclax treatment

Introduction

The median age of onset of Multiple Myeloma (MM), an aggressive cancer of terminally differentiated plasma cells, is approximately 69 years of age(1). While triplet and quadruplet combinations of novel therapies, including immunomodulatory agents and cellular therapies, have improved the therapeutic landscape for MM, outcomes remain suboptimal. Survival rates vary by age and cytogenetic status(2). Patients eligible for Autologous Stem Cell Transplant (ASCT) have a median overall survival (OS) of 8 years(3), while for patients > 75 years this falls to 5 years(4). Therefore, there is an urgent need to identify tolerable targeted agents for the treatment of elderly MM patients.

Reliance on the anti-apoptotic proteins BCL-2, MCL-1 and BCL-XL has emerged as a vulnerability for MM cells(5). The anti-apoptotic BCL-2 proteins (BCL-2, MCL-1, BCL-XL, BFL-1) function by binding and inhibiting the activity of pro-apoptotic proteins (BIM, BAX etc)(6, 7). Due to their function in inhibiting cell death, the anti-apoptotic proteins are attractive therapeutic targets. Previously, it was thought that the pro-survival protein MCL-1 was the main anti-apoptotic protein maintaining the viability of MM cells(8). However, selective MCL-1 inhibitors (AMG-176, S68345) are

associated with potential cardiac toxicity, therefore limiting their clinical utility(9, 10). The selective BCL-2 inhibitor, ABT-199/Venetoclax (ven), is the first BH3 mimetic to be approved by the Federal Drug Administration (FDA) for the treatment of chronic lymphocytic leukemia (CLL) and acute myeloid leukemia (AML) in combination with a demethylating agent(11-13).

BCL-2 dependence in MM was initially identified in a subset of patients, characterized by the presence of a translocation in cyclin D1 (CCND1) t(11;14)(14). This was confirmed across a panel of MM cell lines and primary MM samples, that sensitivity to ven was associated with t(11;14) and correlated with BH3 profiling(15). In the Phase III BELLINI trial, evaluating the combination of ven, dexamethasone and bortezomib in relapsed/refractory (R/R) MM, the patients with t(11;14) translocation were particularly sensitive(16). However, a proportion of patients without the t(11;14) translocation were also sensitive to ven, specifically those with high expression of BCL-2(17). This highlights the need to identify combination treatments that could induce BCL-2 dependence in MM, to broaden the patient population that could be treated with ven, as only 16-24% of patients have a t(11;14) translocation(18).

Venetoclax is FDA-approved for the treatment of AML in combination with the demethylating agent 5-azacytidine (5-aza)(13). 5-aza is a cytosine analogue, that gets incorporated into both DNA and RNA, where it acts as an epigenetic modifier inhibiting DNA methyltransferases, resulting in hypomethylation(19). In AML, ven in combination with 5-aza is well tolerated in elderly patients who were ineligible for intensive induction therapy(13, 20). Previously, it was shown that methylation

regulated BCL-2 expression in mixed lineage leukemia (MLL)(21). Whole exome sequencing analysis of MM revealed mutations in a series of epigenetic modifiers genes including *UTX, MLL, MLL2 and HOX9(22)*. This led us to hypothesize that epigenetic modifiers may induce BCL-2 dependence in MM. Our aim was to perform an unbiased screening approach to identify epigenetic modifiers that could induce BCL-2 dependence in MM cells, thereby sensitizing MM cells to ven to expand the cohort of patients that could be treated with ven.

Methods

For a more detailed description of the materials and methods used in the present study, see supplemental information.

CD138$^+$ cell isolation from primary MM bone marrow samples

Primary MM samples were attained by informed consent from patients from Beaumont Hospital, Dublin, Ireland. Ethical approval was granted from the Beaumont hospital and RCSI ethics committee, study number 19/32. For detailed methods of isolation please see supplementary information.

Cell culture

Multiple Myeloma cell lines (JJN3, KMS18, RPMI-8226, H929, MM1S, KMS27 and U266) were cultured in RPMI 1640 medium supplemented with 10% fetal bovine serum; KMS-12BM is supplemented with 20% fetal bovine serum (Gibco, Invitrogen, Carlsbad, CA, USA), 1% L-Glutamine (2 mM) (Gibco, Invitrogen, Carlsbad, CA, USA) and 1% v/v penicillin/streptomycin (50 units/ml) (Gibco, Invitrogen, Carlsbad, CA, USA). Primary Multiple Myeloma bone marrow stroma cells (MM-BMSC) were

cultured in DMEM medium supplemented with 10% fetal bovine serum (Gibco, Invitrogen, Carlsbad, CA, USA), 1% L-Glutamine (2 mM) (Gibco, Invitrogen, Carlsbad, CA, USA) and 1% v/v penicillin/streptomycin (50 units/ml) (Gibco, Invitrogen, Carlsbad, CA, USA).

Dynamic BH3 profiling

For BH3 profiling, JJN3 cells were seeded at 3 x 10^6 cells in a T25 flask for 24 hrs, cells were treated with 3 μM 5-aza for 20 hrs. Cells were resuspended in 100 μL of buffer (1% FBS 0.4% EDTA (2 mM) in PBS, final pH 7.4) and incubated with a panel of BH3 peptides for 60 min at 21^{o}C (Table 1). Details on the methods are provided in the supplemental Materials and methods.

Data and statistical analyses

GraphPad Prism 9.0 software was used for all statistical analyses. Dose-response curves and IC_{50} values were calculated using linear regression curve fit (Log inhibitor vs. normalized response, variable slope). Unless otherwise stated, the results are expressed as the mean ± standard error of the mean (SEM) of three independent experiments. Webb's fractional product method was used to calculate the synergistic activity of pairs of drugs/inhibitors denoted A and B on cell viability using the following equation: CI = AB/((A*B)/100), where CI > 1.0 indicates antagonistic activity, CI = 1.0 indicates additive interactions, CI < 0.8 indicates strong synergy.

Results

Epigenetic modifier screen to induce BCL-2 dependence and sensitivity to ven.

Taking an unbiased screening approach, we screened 21 epigenetic modifiers, in two non-BCL-2 dependent MM cell lines, to try and induce BCL-2 dependency and enhance sensitivity to ven. We confirmed that JJN3 mainly relied on MCL-1 for survival, as they were most sensitive to AMG-176, a BH3 mimetic that selectively inhibits MCL-1(23). In the BH3 profile, the A12 BH3 peptide that antagonizes MCL-1(24) caused a large reduction in mitochondrial membrane potential (Fig 1A)(25). The KMS18 cell line was mixed BCL-2/BCL-XL dependent as evidenced by sensitivity to ABT-263 that antagonizes BCL-2, BCL-XL and BCL-w (26), and the BH3 peptides BAD and HRK induced loss of mitochondrial membrane potential (Fig 1B)(27). Table 2 contains the list of the epigenetic compounds that were screened in both the KMS18 and JJN3 cell lines using CellTiter-Glo®. The classes of epigenetic modifiers included histone deacetylase inhibitors (HDACi), histone methyltransferase inhibitors (HMTi), DNA methyltransferase inhibitors (DNMTi), histone acetylase inhibitors (HATi) and bromodomain and extra terminal inhibitors (BETi) (Table 2). The 21 epigenetic modifier drugs were screened alone or in combination with ven in the two MM cell lines, at two doses (100 and 500 nM) (Fig 1C and 1D). Based on the initial screen, the top 12 hits were assessed for an ability to induce cell death, as assessed by Annexin V/ Propidium Iodide (PI), in combination with ven in the JJN3 cell line (Fig S2), and the KMS-18 cell line (Fig S3). The hits were ranked based on changes in the area under the curve (AUC) ratio of the epigenetic modifier alone versus the epigenetic modifier and ven (Fig 1E). The lead hits from the cell death analysis in both the JJN3 and KMS18 cell lines were the histone methyltransferase inhibitors, (JIB-04 and GSK-J4), the DNA methyltransferase inhibitor (5-aza), and the

HDAC inhibitor (panobinostat) (Fig 1F and Fig 1G). However, as is evidenced from the dose-response curves (Fig S2 and S3), the top four hits all showed similar enhanced cell death and changes in IC_{50} values upon combination treatment.

5-aza enhanced ven-induced cell death even in the presence of bone marrow stromal cells.

While the lead hits from the screen were the histone demethylase inhibitors those compounds have only been assessed pre-clinically. Excitingly, the combination of 5-aza and ven has not been previously tested in MM, and it has been shown to have acceptable tolerability in elderly AML patients and is FDA-approved as a combination treatment(13). As shown in the JJN3, while ven caused very little cell death alone (IC_{50} 14.2 μM), when combined with 5-aza, there is a log fold change in IC_{50} value (IC_{50} 0.4 μM) (Fig 2A). This is also evident by live cell imaging of the JJN3 cells, with enhanced cell killing in the combination treatment and loss of mitochondrial staining with PK Mito Orange (PKMO)(28) (Fig 2B). Interestingly, although ven did not induce cell death, it did cause a phenotypic change to the mitochondrial structure, as determined by PKMO staining. Next, we assessed the combination of ven + 5-aza in a panel of 5 additional MM cell lines (Fig S4A-F). Remarkably, across the panel of cell lines tested 5-aza significantly altered the IC_{50} value when combined with ven in all 5 cell lines (Fig. 2C). The KMS27 cell line was most sensitive to ven treatment alone, likely because this cell line has a t(11;14) translocation but the addition of 5-aza reduced the IC_{50} by half. The combination index score for synergy is represented as a heatmap in (Fig S4G&H). We also assessed the reverse combination measuring the effect of ven treatment on a 5-aza dose-response curve, with 4/5 of the cell lines showing major changes in IC_{50} values upon the addition of

ven (Fig S4J-N), with combination index scores of synergy graphed as a heatmap (Fig S4O).

The complex interplay between MM cells and the bone marrow microenvironment has been shown to influence cell behavior, particularly MM survival and drug resistance(29). To assess the impact of bone marrow stroma cells on the 5-aza and ven combination, we performed co-culture experiments using HS-5, a bone marrow stroma cell line, and primary MM bone marrow stromal cells (MM-BMSCs) (Fig 2D). Surprisingly, co-culture of JJN3 cells with HS-5 cells conferred significant increase in cell death with 5-aza and ven, compared to JJN3 cells alone (Fig. 2E). Of interest, when MM1S cells were co-cultured with HS-5 cells, they were slightly less sensitive to the 5-aza and ven combination (Fig. 2F). Next, we co-cultured JJN3 cells with MM-BMSCs isolated from a MM patient bone marrow sample (Fig. 2G). The JJN3 cells were still sensitive to 5-aza and ven combination when co-cultured with the MM-BMSCs. In summary, while the MM1S cells benefit from a slight protective effect and the JJN3 cells are slightly sensitized following co-culture with the HS-5 cells, the 5-aza and ven is still an effective treatment combination in the presence of bone marrow stroma cells, across multiple cell lines with diverse anti-apoptotic dependencies.

5-azacytidine induces NOXA through the integrated stress response antagonizing MCL-1, sensitizing MM cells to ven treatment

To understand the mechanism of action of how 5-aza may enhance sensitivity to ven in MM cell lines, a series of approaches were taken. Firstly, we used dynamic BH3 profiling to determine changes in BH3 peptide-induced cytochrome *c* release from mitochondria, following 5-aza treatment (Fig. 3A). As is clear from the BH3 profile,

there was a statistically significant increase in the amount of cytochrome *c* released following the addition of the A12 BH3 peptide, that selectively binds MCL-1, following treatment with 5-aza. In addition, direct ven treatment, as part of the BH3 profile on permeabilized cells, caused a statistically significant increase in the release of cytochrome *c*, following 5-aza treatment in the JJN3 cells (Fig 3A). Next, we confirmed the dynamic BH3 profile by assessing the pro-apoptotic proteins that might be interacting with MCL-1 using immunoprecipitation. Following 5-aza treatment there was an increase in the amount of both BIM EL and NOXA bound to MCL-1 (Fig 3B). Previously, it was shown in AML cells, that 5-aza induced NOXA by the integrated stress response(30). Indeed, we found a similar induction of NOXA following 5-aza treatment in the JJN3 cells, which was even greater in the combination of 5-aza and ven (Fig 3C). We also assessed if this induction of NOXA was dependent on the integrated stress response. Pretreatment with ISRIB, which blocks the integrated stress response by targeting eIF1B(31), also blocked the induction of the NOXA protein following the combination treatment (Fig 3C). Ven alone induces a small amount of NOXA protein, but it enhances the amount of NOXA induced by 5-aza (Fig 3C). We confirmed that ISRIB did not alter eIF2α phosphorylation but prevented the induction of activating transcription factor 4 (ATF-4) by 5-aza and 5-aza+ven (Fig 3D). Confirming the importance of the integrated stress response in the cell death induced by ven + 5-aza, there was a significant reduction in cell death upon pre-treatment with ISRIB (Fig 3E).

There is evidence in the literature that 5-aza can induce dsRNA, through reactivation of endogenous retrovirus(32). Therefore, we assessed the amount of dsRNA in JJN3 cells treated with 5-aza, ven or the combination (Fig 4A). While all treatments induced some dsRNA, the combination of ven + 5-aza induced the most significant

amount, as assessed by pixel count (Fig 4B). Next, we assessed if the knockdown of the dsRNA sensor PKR, which can activate the integrated stress response, could protect from the cell death induced by the combination treatment. Knockdown of *PKR* significantly reduced the cell death induced by the combination treatment (Fig 4C). The densitometry on PKR knockdown is graphed in (Fig S5C). Validating the importance of NOXA in the cell death mechanism, siRNA knockdown of *PMAIP1* (NOXA gene), also significantly protected against the combination induced cell death (Fig 4D). Similarly, densitometry for NOXA knockdown is graphed in (Fig S5D). A proposed model is shown in (Fig 4E). Combined the data suggests the mechanism of synergy following 5-aza + ven, is due at least in part, to an increase in dsRNA, activating PKR, activating the integrated stress response, with an increase in eIF2α phosphorylation, inducing NOXA protein that antagonizes MCL-1. By antagonizing MCL-1, the cells are more sensitive to ven (Fig 4E).

Assessing if a steroid enhances the cell death induced by 5-aza and ven in MM and immune cells.

It is standard practice for a steroid, such as dexamethasone to be added to a combination treatment regimen in MM(33). Therefore, we assessed the combination of ven, 5-aza and dexamethasone in a panel of MM cells. Interestingly, we did not find any significant increase in cell death upon the addition of 1 μM dexamethasone to the combination of ven and 5-aza, across three different MM cell lines (Fig 5A-C). Indeed, the combination of ven and 5-aza caused significantly more cell death than dexamethasone (1 μM) and ven in both the JJN3 and MM1S cell lines (Fig 5A, B). Next, we measured the effect of the combination treatment on immune cells, ven has been shown to induce cell death in B(34) and T cells(35). Using peripheral blood

mononuclear cells from healthy donors, we treated the cells *ex-vivo* for 16 hrs and measured cell death of $CD3^+$ T cells by annexin V/PI staining (Fig 5D). In the $CD3^+$ T cells, 5-aza caused a minimal amount of cell death alone. Ven induced some cell death in $CD3^+$ T cells, as was found previously in mouse $CD8^+$ T cells(35), and additive cell death was seen with the combination treatment of 5-aza and ven (Fig. 5E). The combination of dexamethasone and ven caused slightly more cell death, which was significant, than ven and 5-aza (Fig. 5E). Dexamethasone combined with ven caused a dose-dependent increase in T cell death (Fig 5F). Potentially, the reason for this enhanced cell death is due to dexamethasone inducing a BCL-2 expression in T cells. As can be seen in Fig. 5G-H, there was a dose-dependent increase in BCL-2 expression following dexamethasone treatment, as measured by intercellular BCL-2 staining by flow cytometry. Our data potentially suggests that the addition of a steroid may induce more cell death in the immune cells while having little effect on the tumor cell killing, at least *ex-vivo*. Based on this result, there is a potential to use a steroid-sparing regimen to test the combination of ven/5-aza in the clinic. This steroid effect on T cells may also have implications for the efficacy of many other therapies in MM.

Ven and 5-aza show enhanced killing of primary MM samples irrespective of stage or cytogenetics.

As the combination treatment had only been assessed in MM cell lines, we next wanted to confirm our findings that the combination of 5-aza and ven was effective in heterogeneous MM patient samples. Following isolation of $CD138^+$ patients' cells, the cells were seeded and treated with either increasing doses of BH3 mimetics for

16 hrs or the combination of 5-aza and ven and cell death was measured using Annexin V/PI staining on the flow cytometer (Fig 6A, Fig S6 A-K, Fig S7A-K).

Of the 11 primary MM bone marrow samples analyzed *ex-vivo* (Fig 6A), 8 were non-t(11;14) patients (Table S1). The combination of 5-aza and ven showed enhanced cell killing in 6 out of the 8 non-t(11;14) (Fig 6B) and 2 out of 3 t(11;14) samples (Fig 6C), with 6 samples showing a CI score of less than 1 (Fig S6A-K). Patient cytogenetics were not known at the time of ven treatment. The dose of ven used induced substantial cell death alone in the t(11;14) patient samples, with a statistical difference in the *ex-vivo* sensitivity of non-t(11;14) samples versus the t(11;14) samples (Fig 6D). This data highlights the use of BH3 mimetic profiling as a near-patient test to identify patients who may respond to ven. There was a diverse anti-apoptotic dependence across the MM patient samples (Fig S6). Four of the primary samples $CD138^+$ patient cells were more BCL-2 dependent, four were more MCL-1 dependent and three samples were a mix, with the BCL-XL dependent samples showing the lowest cell death following combination treatment (Fig 6E). Lastly, there was no statistical difference in the combination treatment of ven and 5-aza in upfront versus relapsed patient samples (Fig 6F) or in patients with normal or altered cytogenetics (Fig 6G). Importantly, here we have shown for the first time that 5-aza and ven are effective at killing primary MM samples *ex-vivo*, overcoming high-risk cytogenetic features and multiple lines of prior therapies.

Discussion

Multiple Myeloma is a disease with a diverse genetic background and to date, the development of molecularly targeted therapies has proven elusive. Our aim was to

take an unbiased screening approach to identify epigenetic modifiers that could induce BCL-2 dependence in MM cells to broaden the patient population that could benefit from treatment with ven(15). The DNA methyltransferase inhibitor 5-aza emerged as one of the top hits from our screen. Ven in combination with 5-aza has never been tested in MM, albeit being an approved combination regimen in AML(36). We identified a mechanism of synergism, 5-aza in combination with ven induces NOXA protein inhibiting MCL-1, sensitizing MM cells to ven. The induction of NOXA is reliant on the integrated stress response, with evidence of phosphorylation of eIF2-α. A similar mechanism was identified for 5-aza in AML, ATF4 was responsible for inducing NOXA expression(30). Importantly, we demonstrated that *PMAIP1* (NOXA) knockdown partially rescued the cell death induced by the combination treatment, as did inhibition of the integrated stress response with ISRIB. We also showed for the first time, the translational potential of 5-aza and ven in combination, which demonstrated strong cell killing effect in primary $CD138^+$ MM cells *ex-vivo*, irrespective of cytogenetic background.

In the case of AML, either 5-aza or decitabine were both effective at enhancing the response to ven treatment(13, 20). In contrast, in our study, while 5-aza enhanced the cell death induced by ven, decitabine did not cause a similar enhanced cell death. Decitabine is a deoxyribonucleotide and is incorporated into DNA, whereas 5-aza is a ribonucleoside and is incorporated into both DNA and RNA(19, 37). Potentially, this difference could explain why 5-aza enhances cell death in MM and may suggest the integration into mRNA may lead to activation of the integrated stress response. A series of studies have also shown evidence that 5-aza acts through activation of endogenous retroviral elements (ERVs), inducing viral mimicry and activating the dsRNA sensing pathways (e.g. MDA5, TLR3)(32, 38). We showed

that the combination treatment induced dsRNA in the cells and that knockdown of the dsRNA sensor *PKR*, partially rescued the cell death induced by the combination. We did not investigate if the dsRNA also activates RIG-1 to signal through the mitochondrial antiviral-signaling protein (MAVS), to induce type 1 interferons and proinflammatory cytokines(32, 39). The combination of ven + 5-aza works very effectively in the clinic in AML(13, 36). Activation of the dsRNA pathway by the combination treatment, as shown in our data, could also activate an immune response, this could potentially play an important role in the mechanism of action *in vivo*, however, this was not assessed in this study.

Steroid utilization in MM is standard practice (40). Therefore, we assessed if the addition of the steroid dexamethasone enhanced the cell death induced by the combination treatment (ven + 5-aza). We did not detect any enhanced killing in 3 different MM cell lines, with diverse anti-apoptotic dependence, following the addition of dexamethasone to the combination. The combination of 5-aza + ven was more effective at killing than dex + ven, which was previously identified as an effective combination in MM(41, 42). Potentially, our data may help to explain the latest phase 3 CANOVA trial data with ven and dex in t(11;14) patients, which did not reach a significant endpoint in comparison to pomalidomide + dex, despite evidence of longer progression-free survival(43). Next, we assessed the combination on immune cell killing *ex-vivo* on T cells, as it was previously identified that mature T cells express high BCL-2(27, 44) and are sensitive to ven treatment alone(35, 45). We found a similar induction of cell death in human CD3 T cells with ven treatment alone, and the addition of 5-aza did enhance cell killing. However, dex + ven caused significantly more death of the T-cells than 5-aza + ven, and dexamethasone

induced BCL-2 expression in the CD3 cells. This data would suggest that a steroid has little therapeutic benefit, as it did not enhance the MM cell killing, but it may enhance the killing of immune cells, potentially limiting immune cells' capacity to kill tumor cells(17). In a randomized trial comparing lenalidomide with high-dose versus low-dose dexamethasone, the low-dose dexamethasone regimen was associated with better short-term overall survival(46). Indeed, a high-dose dexamethasone regimen was associated with toxicities, particularly in frail, elderly patients. In a recent abstract, the results of a phase 3 trial comparing daratumumab and lenalidomide without long-term dexamethasone to lenalidomide and dexamethasone were described(47). This trial showed that the overall response rates were higher in the dexamethasone-sparing regimen. This study highlighted that there is a case to not add dexamethasone to MM regimens, particularly in frail, elderly patients with MM, in the situation where the patient is getting highly effective therapy**.**

To assess the translational relevance of 5-aza and ven, we screened the combination in a panel of primary MM CD138+ cells from MM patients, with different cytogenetic backgrounds. In total, 11 patient samples were assessed, 4 were MCL-1 dependent, 3 were mixed anti-apoptotic dependent and 4 samples were BCL-2 dependent. The two samples that did not respond to the combination treatment had a higher sensitivity to the BCL-XL antagonist. Given the mechanism of the synergy described, induction of the NOXA protein binding to MCL-1 could potentially explain the lack of response in these two patient samples. Of the four samples that were BCL-2 dependent, it was later revealed by cytogenetics that 3 had t(11;14) translocation. Gomez-Bougie and colleagues looked at the anti-apoptotic dependence in MM samples(48) and saw that BCL-2 dependence was mostly found in the t(11;14) subgroup and 35% of the samples there was a co-dependency on

either BCL-2/MCL-1 or BCL-XL/MCL-1. While we only assessed a small cohort of samples, the results corroborated previous studies, confirming that there are diverse anti-apoptotic dependencies in MM primary samples(25).

In our study, we used patient-specific sensitivity measurements by carrying out *ex-vivo* functional cell death measurements of primary MM samples treated with BH3 mimetics to determine the anti-apoptotic dependence. Our group has previously identified BCL-2 dependence in a patient with secondary plasma cell leukemia(49). BH3 profiling can also be used to identify resistance mechanisms to ven, including switching of anti-apoptotic dependence(50-53). An important study by Gupta *et al.* used *ex-vivo* assessment of MM patients' samples to ven as an indicator of PFS(54). As we have also shown here, assays such as precision testing and BH3 profiling are dynamic and give a functional measurement of cellular response to treatment and can be useful for *a priori* identifying sensitive patients.

Collectively, our data identifies 5-aza and ven as an effective therapeutic combination for the treatment of MM, including in patients with non-t(11;14) disease with high-risk cytogenetics such as 17p and 1q amplification. This combination has the potential to be effective across a broad patient population and should be considered in a steroid-free regimen for assessment in a clinical trial setting.

References

1. Cancer Factsheet Multiple Myeloma (ICD-10 C90) NCRI. 28th June 2023. Available from: https://www.ncri.ie/factsheets.

2. Rajkumar SV. Multiple myeloma: 2020 update on diagnosis, risk-stratification and management. Am J Hematol. 2020;95(5):548-567.

3. Landgren O, Weiss BM. Patterns of monoclonal gammopathy of undetermined significance and multiple myeloma in various ethnic/racial groups: support for genetic factors in pathogenesis. Leukemia. 2009;23(10):1691-1697.

4. Moreau P, Attal M, Facon T. Frontline therapy of multiple myeloma. Blood. 2015;125(20):3076-3084.

5. Maji S, Panda S, Samal SK, et al. Bcl-2 Antiapoptotic Family Proteins and Chemoresistance in Cancer. Adv Cancer Res. 2018;137:37-75.

6. Ni Chonghaile T, Letai A. Mimicking the BH3 domain to kill cancer cells. Oncogene. 2008;27 Suppl 1:S149-157.

7. Cory S, Adams JM. The Bcl2 family: regulators of the cellular life-or-death switch. Nat Rev Cancer. 2002;2(9):647-656.

8. Wuilleme-Toumi S, Robillard N, Gomez P, et al. Mcl-1 is overexpressed in multiple myeloma and associated with relapse and shorter survival. Leukemia. 2005;19(7):1248-1252.

9. Thomas RL, Roberts DJ, Kubli DA, et al. Loss of MCL-1 leads to impaired autophagy and rapid development of heart failure. Genes Dev. 2013;27(12):1365-1377.

10. Wang X, Bathina M, Lynch J, et al. Deletion of MCL-1 causes lethal cardiac failure and mitochondrial dysfunction. Genes Dev. 2013;27(12):1351-1364.

11. Roberts AW, Davids MS, Pagel JM, et al. Targeting BCL2 with Venetoclax in Relapsed Chronic Lymphocytic Leukemia. N Engl J Med. 2016;374(4):311-322.

12. DiNardo CD, Stein EM, de Botton S, et al. Durable Remissions with Ivosidenib in IDH1-Mutated Relapsed or Refractory AML. N Engl J Med. 2018;378(25):2386-2398.

13. DiNardo CD, Pratz K, Pullarkat V, et al. Venetoclax combined with decitabine or azacitidine in treatment-naive, elderly patients with acute myeloid leukemia. Blood. 2019;133(1):7-17.

14. Bodet L, Gomez-Bougie P, Touzeau C, et al. ABT-737 is highly effective against molecular subgroups of multiple myeloma. Blood. 2011;118(14):3901-3910.

15. Touzeau C, Dousset C, Le Gouill S, et al. The Bcl-2 specific BH3 mimetic ABT-199: a promising targeted therapy for t(11;14) multiple myeloma. Leukemia. 2014;28(1):210-212.

16. Kumar S, Kaufman JL, Gasparetto C, et al. Efficacy of venetoclax as targeted therapy for relapsed/refractory t(11;14) multiple myeloma. Blood. 2017;130(22):2401-2409.

17. Kumar S, Harrison SJ, Cavo M, et al. Final Overall Survival Results from BELLINI, a Phase 3 Study of Venetoclax or Placebo in Combination with Bortezomib and Dexamethasone in Relapsed/Refractory Multiple Myeloma. Blood. 2021;138(Supplement 1):84-84.

18. Bal S, Kumar SK, Fonseca R, et al. Multiple myeloma with t(11;14): unique biology and evolving landscape. Am J Cancer Res. 2022;12(7):2950-2965.

19. Stresemann C, Lyko F. Modes of action of the DNA methyltransferase inhibitors azacytidine and decitabine. Int J Cancer. 2008;123(1):8-13.

20. DiNardo CD, Pratz KW, Letai A, et al. Safety and preliminary efficacy of venetoclax with decitabine or azacitidine in elderly patients with previously untreated acute myeloid leukaemia: a non-randomised, open-label, phase 1b study. Lancet Oncol. 2018;19(2):216-228.

21. Benito JM, Godfrey L, Kojima K, et al. MLL-Rearranged Acute Lymphoblastic Leukemias Activate BCL-2 through H3K79 Methylation and Are Sensitive to the BCL-2-Specific Antagonist ABT-199. Cell Rep. 2015;13(12):2715-2727.

22. Palumbo A, Anderson K. Multiple myeloma. N Engl J Med. 2011;364(11):1046-1060.

23. Caenepeel S, Brown SP, Belmontes B, et al. AMG 176, a Selective MCL1 Inhibitor, Is Effective in Hematologic Cancer Models Alone and in Combination with Established Therapies. Cancer Discov. 2018;8(12):1582-1597.

24. Foight GW, Ryan JA, Gulla SV, Letai A, Keating AE. Designed BH3 peptides with high affinity and specificity for targeting Mcl-1 in cells. ACS Chem Biol. 2014;9(9):1962-1968.

25. Touzeau C, Ryan J, Guerriero J, et al. BH3 profiling identifies heterogeneous dependency on Bcl-2 family members in multiple myeloma and predicts sensitivity to BH3 mimetics. Leukemia. 2016;30(3):761-764.

26. Tse C, Shoemaker AR, Adickes J, et al. ABT-263: a potent and orally bioavailable Bcl-2 family inhibitor. Cancer Res. 2008;68(9):3421-3428.

27. Chonghaile TN, Roderick JE, Glenfield C, et al. Maturation stage of T-cell acute lymphoblastic leukemia determines BCL-2 versus BCL-XL dependence and sensitivity to ABT-199. Cancer Discov. 2014;4(9):1074-1087.

28. Liu T, Stephan T, Chen P, et al. Multi-color live-cell STED nanoscopy of mitochondria with a gentle inner membrane stain. Proc Natl Acad Sci U S A. 2022;119(52):e2215799119.

29. Vincent T, Mechti N. Extracellular matrix in bone marrow can mediate drug resistance in myeloma. Leuk Lymphoma. 2005;46(6):803-811.

30. Jin S, Cojocari D, Purkal JJ, et al. 5-Azacitidine Induces NOXA to Prime AML Cells for Venetoclax-Mediated Apoptosis. Clin Cancer Res. 2020;26(13):3371-3383.

31. Sidrauski C, Acosta-Alvear D, Khoutorsky A, et al. Pharmacological brake-release of mRNA translation enhances cognitive memory. Elife. 2013;2:e00498.

32. Chiappinelli KB, Strissel PL, Desrichard A, et al. Inhibiting DNA Methylation Causes an Interferon Response in Cancer via dsRNA Including Endogenous Retroviruses. Cell. 2015;162(5):974-986.

33. Shah UA, Mailankody S. Emerging immunotherapies in multiple myeloma. BMJ. 2020;370:m3176.

34. Khaw SL, Merino D, Anderson MA, et al. Both leukaemic and normal peripheral B lymphoid cells are highly sensitive to the selective pharmacological inhibition of prosurvival Bcl-2 with ABT-199. Leukemia. 2014;28(6):1207-1215.

35. Ludwig LM, Hawley KM, Banks DB, et al. Venetoclax imparts distinct cell death sensitivity and adaptivity patterns in T cells. Cell Death Dis. 2021;12(11):1005.

36. DiNardo CD, Rausch CR, Benton C, et al. Clinical experience with the BCL2-inhibitor venetoclax in combination therapy for relapsed and refractory acute myeloid leukemia and related myeloid malignancies. Am J Hematol. 2018;93(3):401-407.

37. Yoo CB, Jones PA. Epigenetic therapy of cancer: past, present and future. Nat Rev Drug Discov. 2006;5(1):37-50.

38. Roulois D, Loo Yau H, Singhania R, et al. DNA-Demethylating Agents Target Colorectal Cancer Cells by Inducing Viral Mimicry by Endogenous Transcripts. Cell. 2015;162(5):961-973.

39. Patel JR, Jain A, Chou YY, et al. ATPase-driven oligomerization of RIG-I on RNA allows optimal activation of type-I interferon. EMBO Rep. 2013;14(9):780-787.

40. Rajkumar SV, Kumar S. Multiple myeloma current treatment algorithms. Blood Cancer J. 2020;10(9):94.

41. Matulis SM, Gupta VA, Nooka AK, et al. Dexamethasone treatment promotes Bcl-2 dependence in multiple myeloma resulting in sensitivity to venetoclax. Leukemia. 2016;30(5):1086-1093.

42. Matulis SM, Gupta VA, Neri P, et al. Functional profiling of venetoclax sensitivity can predict clinical response in multiple myeloma. Leukemia. 2019;33(5):1291-1296.

43. AbbVie presents results from phase 3 CANOVA study of venetoclax in patients with relapsed or refractory multiple myeloma. News release. AbbVie. September 29.

Last accessed 3rd December 2023. Available from: https://news.abbvie.com/2023-09-29-AbbVie-Presents-Results-from-Phase-3-CANOVA-Study-of-Venetoclax-in-Patients-with-Relapsed-or-Refractory-Multiple-Myeloma.

44. Veis DJ, Sentman CL, Bach EA, Korsmeyer SJ. Expression of the Bcl-2 protein in murine and human thymocytes and in peripheral T lymphocytes. J Immunol. 1993;151(5):2546-2554.

45. Rohner L, Reinhart R, Iype J, et al. Impact of BH3-mimetics on Human and Mouse Blood Leukocytes: A Comparative Study. Sci Rep. 2020;10(1):222.

46. Rajkumar SV, Jacobus S, Callander NS, et al. Lenalidomide plus high-dose dexamethasone versus lenalidomide plus low-dose dexamethasone as initial therapy for newly diagnosed multiple myeloma: an open-label randomised controlled trial. Lancet Oncol. 2010;11(1):29-37.

47. Manier S, Corre J, Hulin C, et al. A dexamethasone-sparing regimen with daratumumab and lenalidomide in frail patients with newly-diagnosed multiple myeloma: Efficacy and safety analysis of the phase 3 IFM2017-03 trial. Blood. 2022;140(Supplement 1):1369-1370.

48. Gomez-Bougie P, Maiga S, Tessoulin B, et al. BH3-mimetic toolkit guides the respective use of BCL2 and MCL1 BH3-mimetics in myeloma treatment. Blood. 2018;132(25):2656-2669.

49. Glavey SV, Flanagan L, Bleach R, et al. Secondary plasma cell leukaemia treated with single agent venetoclax. Br J Haematol. 2020;190(4):e242-e245.

50. Di Grande A, Peirs S, Donovan PD, et al. The spleen as a sanctuary site for residual leukemic cells following ABT-199 monotherapy in ETP-ALL. Blood Adv. 2021;5(7):1963-1976.

51. Sullivan GP, Flanagan L, Rodrigues DA, Ni Chonghaile T. The path to venetoclax resistance is paved with mutations, metabolism, and more. Sci Transl Med. 2022;14(674):eabo6891.

52. Ni Chonghaile T, Sarosiek KA, Vo TT, et al. Pretreatment mitochondrial priming correlates with clinical response to cytotoxic chemotherapy. Science. 2011;334(6059):1129-1133.

53. Bhatt S, Pioso MS, Olesinski EA, et al. Reduced Mitochondrial Apoptotic Priming Drives Resistance to BH3 Mimetics in Acute Myeloid Leukemia. Cancer Cell. 2020;38(6):872-890.e6.

54. Gupta VA, Matulis SM, Barwick BG, et al. Venetoclax ex vivo functional profiling predicts improved progression-free survival. Blood Cancer J. 2022;12(8):115.

Peptide	Sequence	Interacts
BIM	MRPEIWIAQELRRIGDEFNA	BAX; BAK; BCL-2; BCL-XL;BCL-w; MCL-1; A1
BAD	LWAAQRYGRELRRMSDEFEGSFKGL	BCL-2; BCL-XL;BCL-w
A12	RPEIWMGQLRRLGDEINAYYAR	MCL-1
HRK	WSSAAQLTAARLKALGDELHQ	BCL-XL
PUMA	EQWAREIGAQLRRMADDLNA	BCL-2; BCL-XL;BCL-w; MCL-1; A1
NOXA	AELPPEFAAQLRKIGDKVYC	MCL-1 at lowest ; at higher doses BCL-2; BCL-XL, BCL-w

Table 1. List of BH3 peptides and interactions with BCL-2 proteins. The BH3 peptides sequence is described along with the pro- and anti-apoptotic proteins that the BH3 peptides bind to.

Class of epigenetic modifier	Drugs
Histone deacetylase inhibitors (HDACi)	Panobinostat (pan-HDACi), belinostat (pan-HDACi), ricolinostat (HDAC6), citarinostat (HDAC6), tacedinaline (HDAC1/2/3), BAS-2 (HDAC6), entinostat (HDAC1/2/3), vorinostat (pan-HDACi)
Histone methyltransferase inhibitors (HMTi)	JIB-04 (Jumonji histone demethylases), GSK-K4 (JMJD3/UTX), pargylcine (MAO-A/B), clorgyline (MAO-A), tranylcypromine (LSD1/MAO-A/B)
Histone acetyltransferase inhibitors (HATi)	Curcumin (p300/CBP), C646 (p300)
DNA methyltransferase inhibitors (DNMTi)	5-azacytidine (DNMT1), decitabine (DNMT1)
Bromodomain and extra terminal inhibitors (BETi)	JQ-1(BRD2/3/4), I-BET-151 (BRD2/3/4), CPI203 (BRD4), UNC-1215 (L3MBTL3)

Table 2. List of epigenetic modifiers. Listed are the types of epigenetic modifiers and drugs in each class used in the screen. They were used at two doses 100 nM and 500 nM in the initial screen.

Figure Legends

Figure 1. Screening epigenetic modifiers in combination with ven in MM cell lines. The area under the curve of the dose-response to BH3 mimetics ABT-199, ABT-263, WEHI-539 and AMG-176 is plotted following 24 hr treatment as measured by Annexin V/PI. The BH3 profiles of JJN3 A) and KMS18 B) are graphed. The mitochondrial membrane potential was measured using JC-1 following exposure to BH3 peptides and BH3 mimetics over 180 min. Graphed is the median ± SEM of three independent experiments. The JJN3 C) and the KMS18 D) cells were treated for 24 hrs with epigenetic modifiers +/- ven. Cells were treated with 2 doses of epigenetic modifier alone, 100 nM and 500 nM, or in combination with 1 μM ven JJN3 cells or 500 nM ven in KMS18 cells for 24 hours. Cell viability was assessed following treatment using Cell Titer Glo® and data was graphed using GraphPad prism. The 12 epigenetic modifier hits from F) JJN3 and G) KMS18 were assessed for cell death by Annexin V/PI staining. Cells were treated with 30 nM, 100 nM, 300 nM, 1 μM and 3 μM of each epigenetic modifier alone and 1 μM ven in JJN3 cells and 500 nM ven in KMS18 cells for 24 hours. The dose-response curves were graphed in Graphpad and the ratio of area under the curve values, as shown in E) were calculated and graphed for each drug in combination with ven.

Figure 2. Assessing the effect of bone marrow stroma cells on the combination of 5-aza and ven in MM cell lines. A) Cell viability was assessed in JJN3 cells using Annexin V/PI staining following 24 hour treatment with dose response of ven +/- 5-aza 3 μM B) Live cell confocal imaging of JJN3 cells following treatment with DMSO, 3 μM 5-azacytidine +/- 1 μM ven for 24 hours. Mitochondria were stained

with PKMO and DNA stained with Picogreen, 5 images were taken per treatment condition, with images representative of three independent experiments. C) The combination treatment was assessed in a panel of MM cell lines by measuring Annexin V/PI positivity by flow cytometry following 24 hrs of treatment. Sensitivity was expressed as IC_{50} μM for ven alone or ven + 5-aza as determined by GraphPad. D) Schematic of the workflow of the co-culture experiments. HS-5 cells or MM-BMSC from an MM patient sample were seeded for 24 hrs. MM cells were co-cultured for 24 hrs and then treated with drugs for 24 hrs before assessment by flow cytometry. E) JJN3 cells were seeded alone (orange) or co-cultured with HS-5 cells for 24 hrs (maroon). The cells were then treated with either 5-aza (1 μM or 3 μM) alone or combined with 1 μM ven (shown by the plus symbol) for 24 hrs. The % cell death of tumour cells was assessed by Annexin V/PI staining on the flow cytometer. F) The same experiment was carried out for the MM1S cells, seeded alone (purple) or co-cultured with HS-5 (maroon) for 24 hrs before treatment. The cells were then treated with either 5-aza (1 μM or 3 μM) alone or combined with 1 μM ven (shown by the plus symbol) for 24 hrs. G) The same experiment as described for E) was carried out with JJN3 cells co-cultured with MM-BMSC cells. Graphed are the median values ± SEM from three independent experiments. Two-way ANOVA with Bonferroni multiple comparison test was used to calculate *p* values. Differences are indicated: ns not significant, ** $p \leq 0.01$ and *** $p \leq 0.001$.

Figure 3. 5-azacytidine increases NOXA expression through the integrated stress response antagonizing MCL-1. A) The effect of 5-aza 3 μM treatment on JJN3 cells after 24 hrs was assessed by dynamic BH3 profiling as described in the materials and methods. B) JJN3 cells were treated with 5-aza 3 μM for 24 hrs. The

association of NOXA and BIM with MCL-1 was determined by immunoprecipitation and Western blot analysis C) JJN3 cells were treated with 3 μM 5-aza; ven 1 μM; (3 μM 5-aza + ven1 μM); (3 μM 5-aza + ven1 μM + 500 nM ISRIB) for 24 hrs and the expression of BCL-2, MCL-1, NOXA, DNMT1 and β-actin were determined by Western blot analysis. D) Cells were treated as in C for 6 hr and expression of p-eIF2α, total eIF2α, ATF4 and β-actin was measured by Western blot E) Cell viability was assessed in JJN3 cells by Annexin V/PI staining following treatment with 3 μM 5-aza; (3 μM 5-aza + ven1 μM); (3 μM 5-aza + ven1 μM + 500 nM ISRIB) for 24 hrs. The mean of three independent experiments +/- SD is graphed.

Figure 4. 5-azacytidine increases dsRNA and the knockdown of PKR protects against the combination treatment. A) JJN3 cells were treated with 3 μM 5-aza, 1 μM ven and (3 μM 5-aza + 1 μM ven), for 24 hr before confocal imaging with DAPI stain for nucleus, MitoTracker™ (deep red FM) for mitochondria and dsRNA for double-stranded RNA. The images are representative of three independent experiments. B) The pixel count for dsRNA is graphed for the three independent experiments for the treatments described in A). C) Cell viability was assessed using Annexin V/PI staining by flow cytometry following control or siRNA to PKR with the following treatments 1 μM ven; 3 μM 5-aza; (3 μM 5-aza + 1 μM ven). The Western blot shows the expression of PKR, with actin as a loading control D) Cell viability was assessed using Annexin V/PI staining by flow cytometry following control or siRNA to NOXA with the treatments listed in D). The Western blot shows the expression of NOXA, with actin as a loading control. E) A graphical model showing the induction of dsRNA activating PKR, knockdown of PKR, NOXA with siRNA or pretreatment with

ISRIB all inhibited the cell death induced by 5-aza + ven. Differences statistically significant are indicated: ** $p \leq 0.01$ and *** $p \leq 0.001$.

Figure 5. Dexamethasone does not enhance ven + 5-aza cell death and induces T-cell death. A) JJN3 cells were treated with 1 μM ven; 3 μM 5-aza; 1 μM dex; (1 μM ven + 1 μM dex); (1 μM ven + 3 μM 5-aza); (1 μM ven + 3 μM 5-aza + 1 μM dex) for 24 hours. Cell viability was measured using Annexin V/PI staining. The mean of three independent repeats is graphed +/- SD. B) MMIS cells were treated with 1 μM ven; 3 μM 5-aza; 1 μM dex; (1 μM ven + 1 μM dex); (1 μM ven + 3 μM 5-aza); (1 μM ven + 3 μM 5-aza + 1 μM dex) for 24 hours. Cell viability was assessed as in A). C) KMS12BM were treated with 0.5 μM ven; 3 μM 5-aza; 1 μM dex; (0.5 μM ven + 3 μM 5-aza); (0.5 μM ven + 3 μM 5-aza + 1 μM dex) for 24 hours. Cell viability was assessed and graphed as in A). D) Schematic of gating strategy used for identifying CD3 T cells. E) Cell viability was assessed in CD3+ T cells isolated from PBMCs using Annexin V/PI staining following 16-hour treatment with 3 μM 5-aza; 300 nM ven; 1 μM dex; (300 nM ven + 3 μM 5-aza); (1 μM Dex + 300 nM Ven) graphed are the mean of three independent experiments E) Cell viability was assessed in CD3+ T following treatment with ven at 100 nM and 300 nM with and without Dex 1 μM Dex. Graphed are the mean of two independent experiments +/- SD. Intracellular BCL-2 staining was measured in T cells following 16-hour treatment with 300 nM, 1 μM and 3 μM Dex. A one-way ANOVA statistical test was performed to determine *p* values: ns not significant ** $p \leq 0.01$ and *** $p \leq 0.001$.

Figure 6. Ven and 5-aza in combination enhance cell death in primary MM samples *ex-vivo.* Cell viability was assessed using Annexin V/PI staining following

16-hour treatment. A) Schematic of the workflow of isolating CD138+ cells from patient bone marrow samples and treating them *ex-vivo.* B) Summary of the response across the 8 non t(11;14) patients to 3 μM 5-aza, 300 nM ven, or combination. C) Summary of the response across 3 t(11;14) patients to 5-aza, ven or in combination. D) Response of non-t (11;14) vs t(11;14) patients to 300 nM ven following 16-hour treatment. Summary of response to 5-aza and ven in 11 patients across E) anti-apoptotic dependencies F) diagnosis and G) cytogenetics.

Figure 1

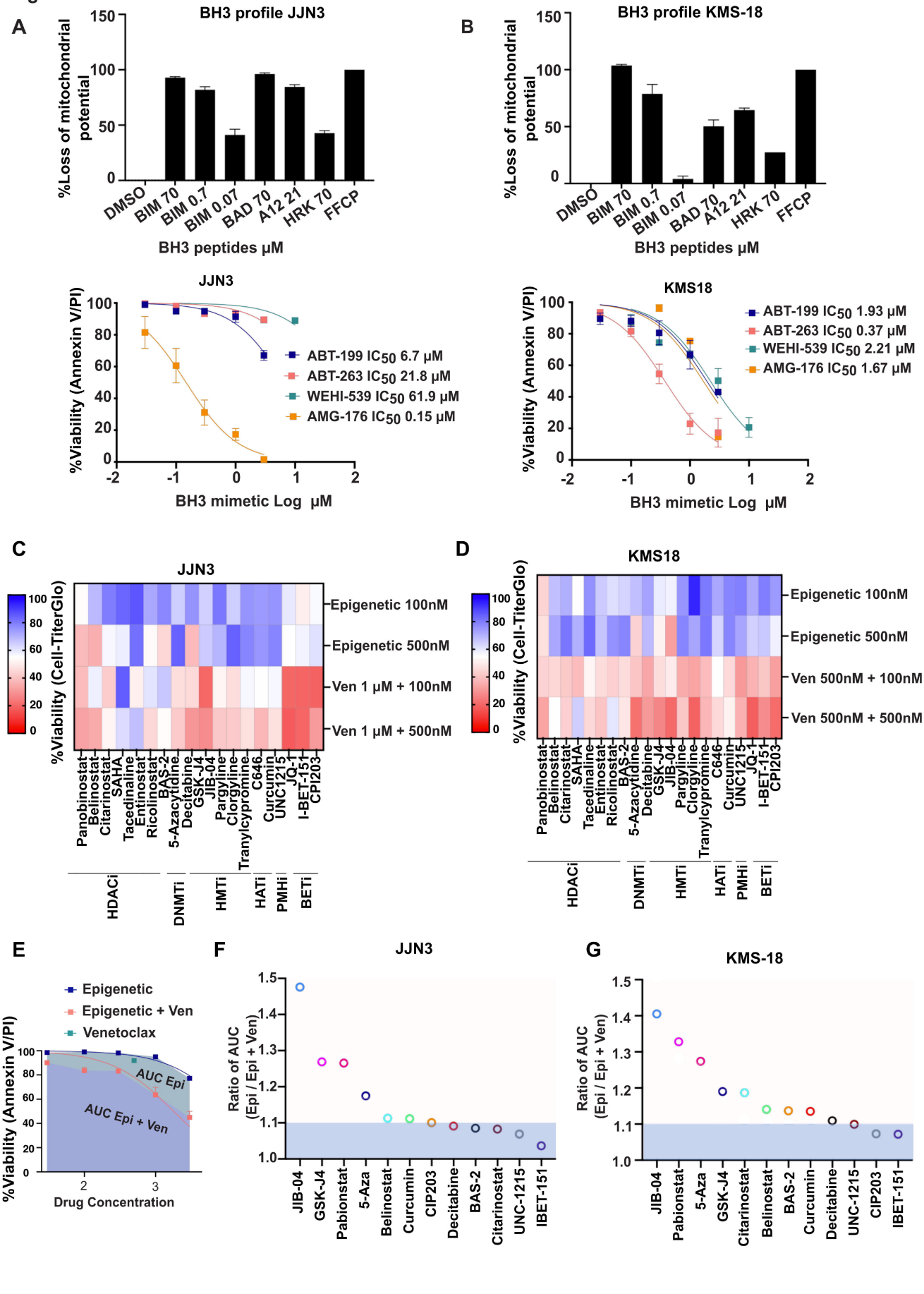
A
BH3 profile JJN3
%Loss of mitochondrial potential
DMSO
BIM 70
BIM 0.7
BIM 0.07
BAD 70
A12 21
HRK 70
FFCP
BH3 peptides µM
B
BH3 profile KMS-18
%Loss of mitochondrial potential
BH3 peptides µM
JJN3
%Viability (Annexin V/PI)
ABT-199 IC50 6.7 µM
ABT-263 IC50 21.8 µM
WEHI-539 IC50 61.9 µM
AMG-176 IC50 0.15 µM
BH3 mimetic Log µM
KMS18
ABT-199 IC50 1.93 µM
ABT-263 IC50 0.37 µM
WEHI-539 IC50 2.21 µM
AMG-176 IC50 1.67 µM
BH3 mimetic Log µM
C
JJN3
%Viability (Cell-TiterGlo)
Epigenetic 100nM
Epigenetic 500nM
Ven 1 µM + 100nM
Ven 1 µM + 500nM
Panobinostat
Belinostat
Citarinostat
SAHA
Tacedinaline
Entinostat
Ricolinostat
BAS-2
5-Azacytidine
Decitabine
GSK-J4
JIB-04
Pargyline
Clorgyline
Tranylcypromine
C646
Curcumin
UNC1215
JQ-1
I-BET-151
CPI203
HDACi
DNMTi
HMTi
HATi
PMHi
BETi
D
KMS18
%Viability (Cell-TiterGlo)
Epigenetic 100nM
Epigenetic 500nM
Ven 500nM + 100nM
Ven 500nM + 500nM
HDACi
DNMTi
HMTi
HATi
PMHi
BETi
E
Epigenetic
Epigenetic + Ven
Venetoclax
%Viability (Annexin V/PI)
AUC Epi
AUC Epi + Ven
Drug Concentration
F
JJN3
Ratio of AUC (Epi / Epi + Ven)
JIB-04
GSK-J4
Pabionstat
5-Aza
Belinostat
Curcumin
CIP203
Decitabine
BAS-2
Citarinostat
UNC-1215
IBET-151
G
KMS-18
Ratio of AUC (Epi / Epi + Ven)
JIB-04
Pabionstat
5-Aza
GSK-J4
Citarinostat
Belinostat
BAS-2
Curcumin
Decitabine
UNC-1215
CIP203
IBET-151

Figure 2

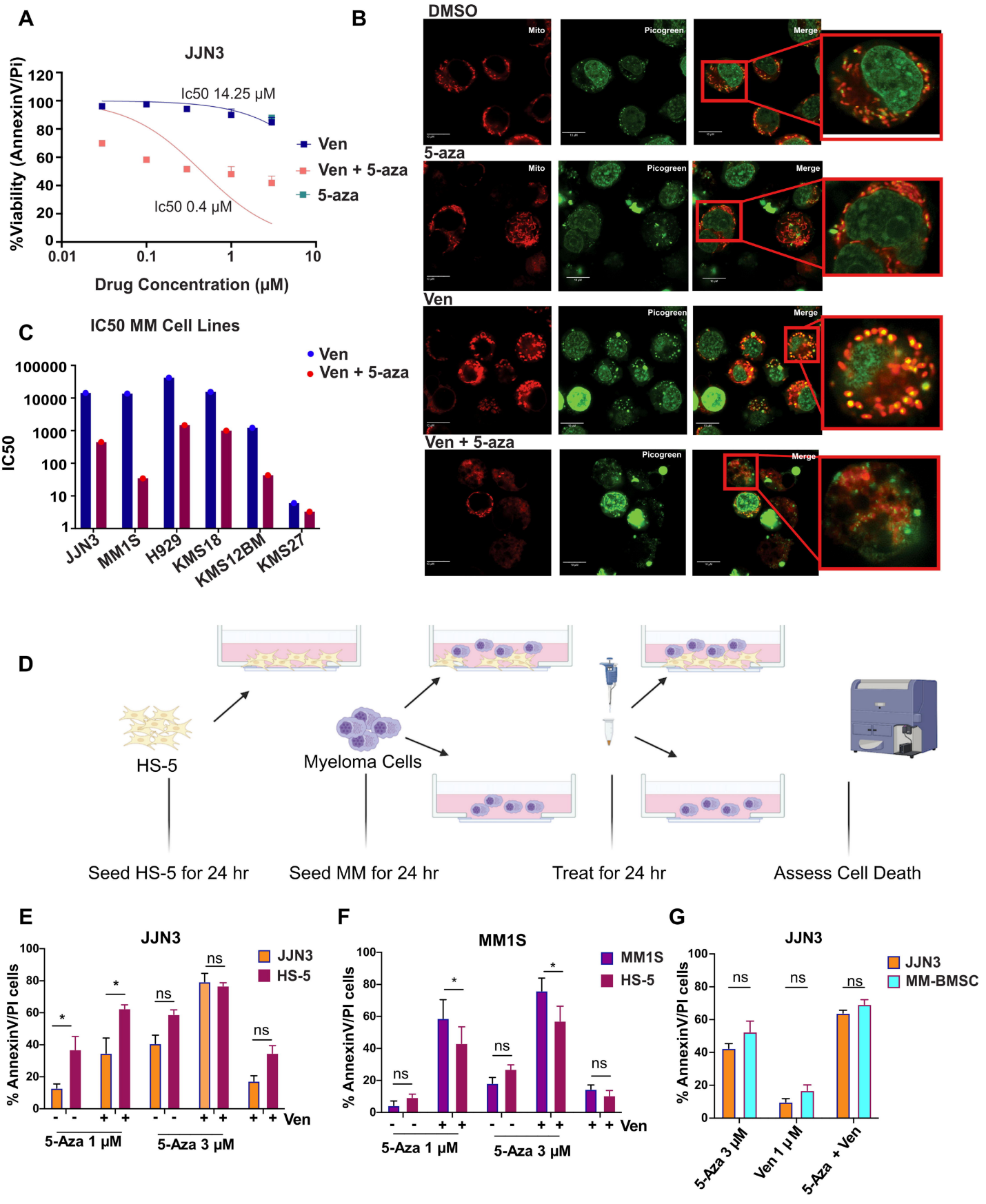
A
JJN3
%Viability (AnnexinV/Pi)
Ic50 14.25 µM
Ic50 0.4 µM
Ven
Ven + 5-aza
5-aza
Drug Concentration (µM)
B
DMSO
5-aza
Ven
Ven + 5-aza
Mito
Picogreen
Merge
C
IC50 MM Cell Lines
IC50
Ven
Ven + 5-aza
JJN3
MM1S
H929
KMS18
KMS12BM
KMS27
D
HS-5
Myeloma Cells
Seed HS-5 for 24 hr
Seed MM for 24 hr
Treat for 24 hr
Assess Cell Death
E
JJN3
% AnnexinV/PI cells
JJN3
HS-5
Ven
5-Aza 1 µM
5-Aza 3 µM
F
MM1S
% AnnexinV/PI cells
MM1S
HS-5
Ven
5-Aza 1 µM
5-Aza 3 µM
G
JJN3
% AnnexinV/PI cells
JJN3
MM-BMSC
5-Aza 3 µM
Ven 1 µM
5-Aza + Ven

Figure 3

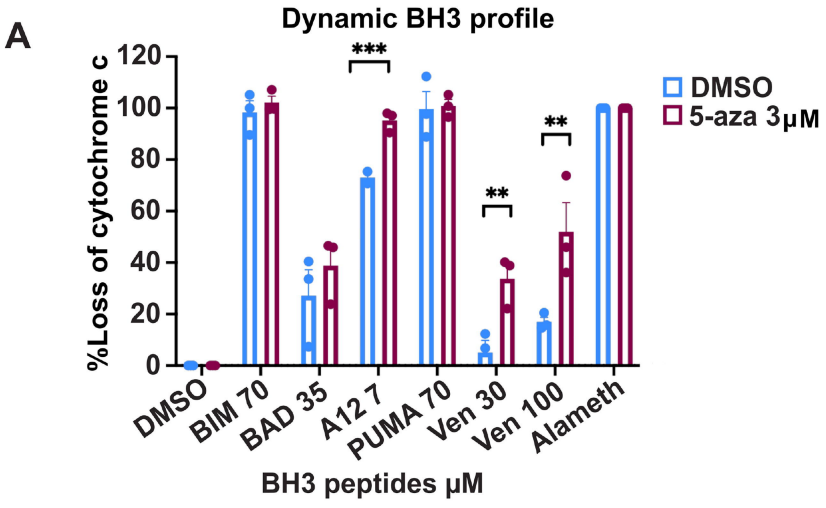
A
Dynamic BH3 profile
%Loss of cytochrome c
120
100
80
60
40
20
0
***
**
**
DMSO
5-aza 3μM
DMSO
BIM 70
BAD 35
A12 7
PUMA 70
Ven 30
Ven 100
Alameth
BH3 peptides μM

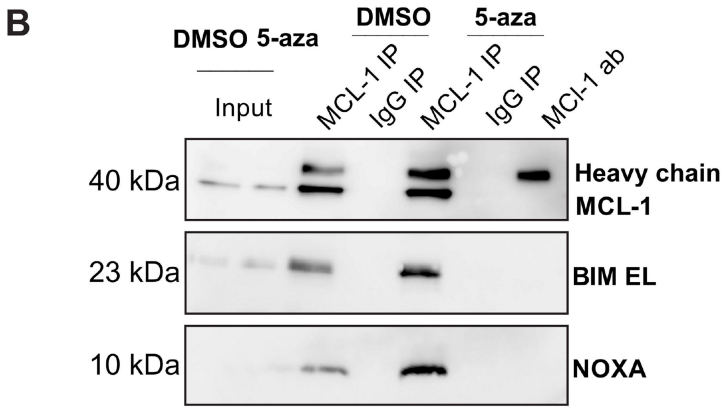
B
DMSO 5-aza
DMSO
5-aza
Input
MCL-1 IP
IgG IP
MCL-1 IP
IgG IP
MCl-1 ab
40 kDa
Heavy chain
MCL-1
23 kDa
BIM EL
10 kDa
NOXA

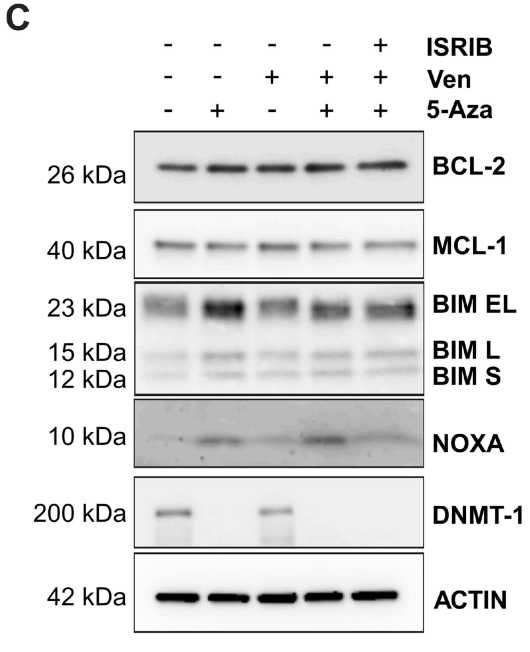
C
ISRIB
Ven
5-Aza
26 kDa
BCL-2
40 kDa
MCL-1
23 kDa
BIM EL
15 kDa
12 kDa
BIM L
BIM S
10 kDa
NOXA
200 kDa
DNMT-1
42 kDa
ACTIN

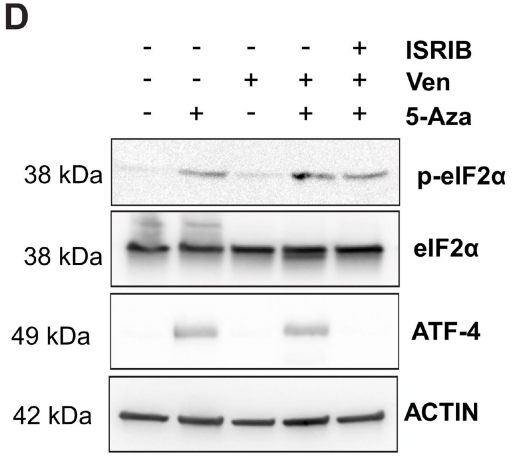
D
ISRIB
Ven
5-Aza
38 kDa
p-eIF2α
38 kDa
eIF2α
49 kDa
ATF-4
42 kDa
ACTIN

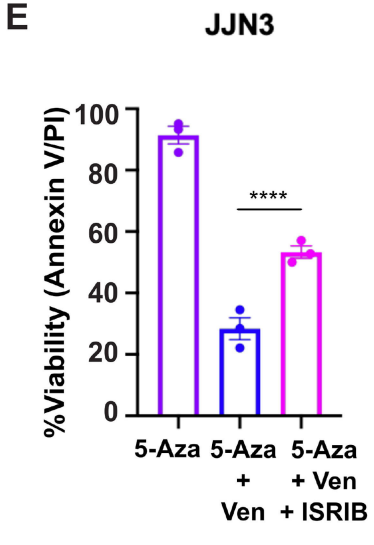
E
JJN3
%Viability (Annexin V/PI)
100
80
60
40
20
0
****
5-Aza
5-Aza + Ven
5-Aza + Ven + ISRIB

Figure 4

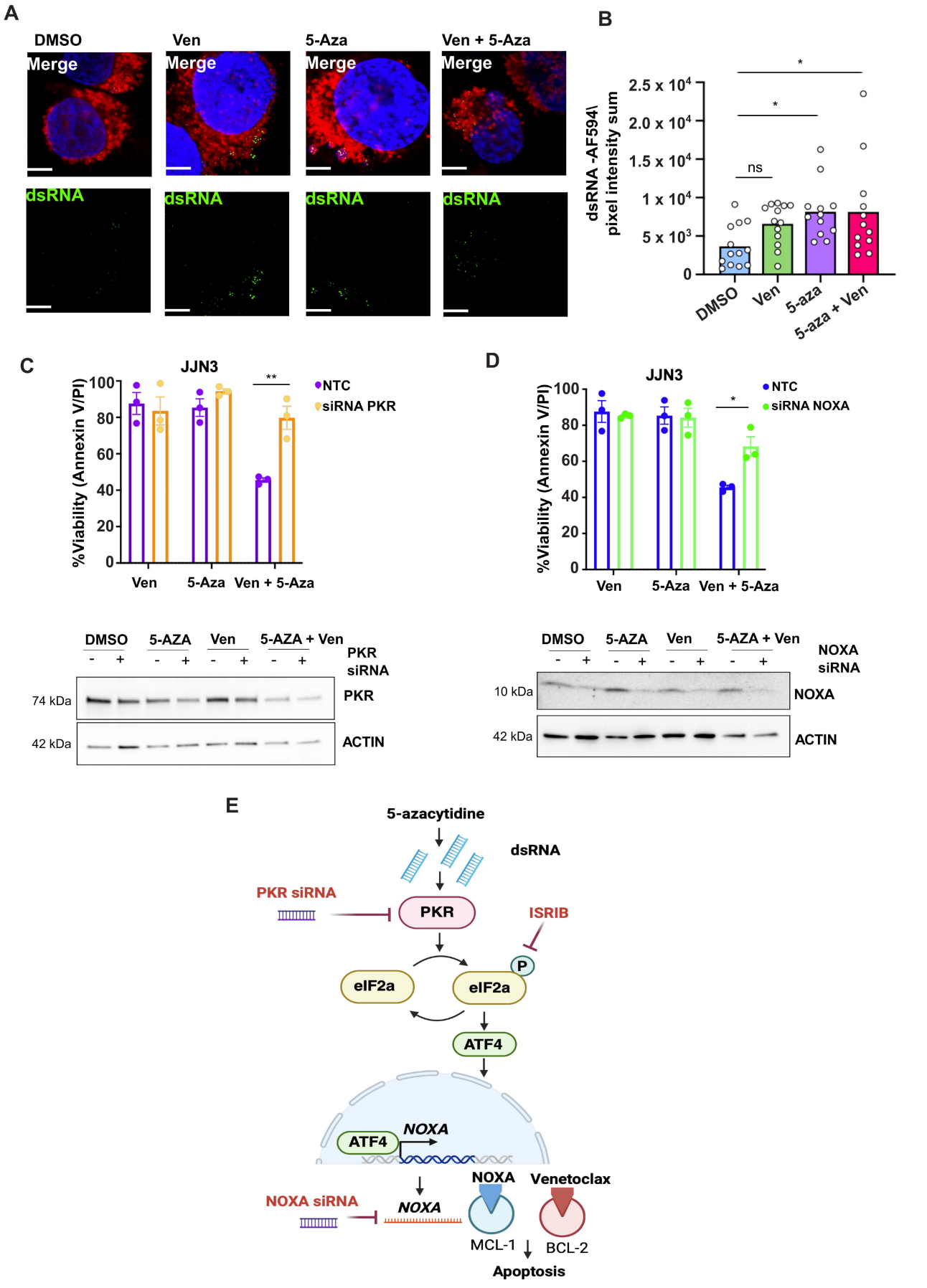
A
DMSO
Ven
5-Aza
Ven + 5-Aza
Merge
dsRNA
B
dsRNA -AF594\ pixel intensity sum
2.5 x 10^4
2.0 x 10^4
1.5 x 10^4
1 x 10^4
5 x 10^3
0
ns
*
DMSO
Ven
5-aza
5-aza + Ven
C
JJN3
%Viability (Annexin V/PI)
NTC
siRNA PKR
**
Ven
5-Aza
Ven + 5-Aza
D
JJN3
%Viability (Annexin V/PI)
NTC
siRNA NOXA
*
Ven
5-Aza
Ven + 5-Aza
DMSO
5-AZA
Ven
5-AZA + Ven
PKR siRNA
74 kDa
PKR
42 kDa
ACTIN
NOXA siRNA
10 kDa
NOXA
E
5-azacytidine
dsRNA
PKR siRNA
PKR
ISRIB
P
eIF2a
ATF4
NOXA
NOXA siRNA
Venetoclax
MCL-1
BCL-2
Apoptosis

Figure 5

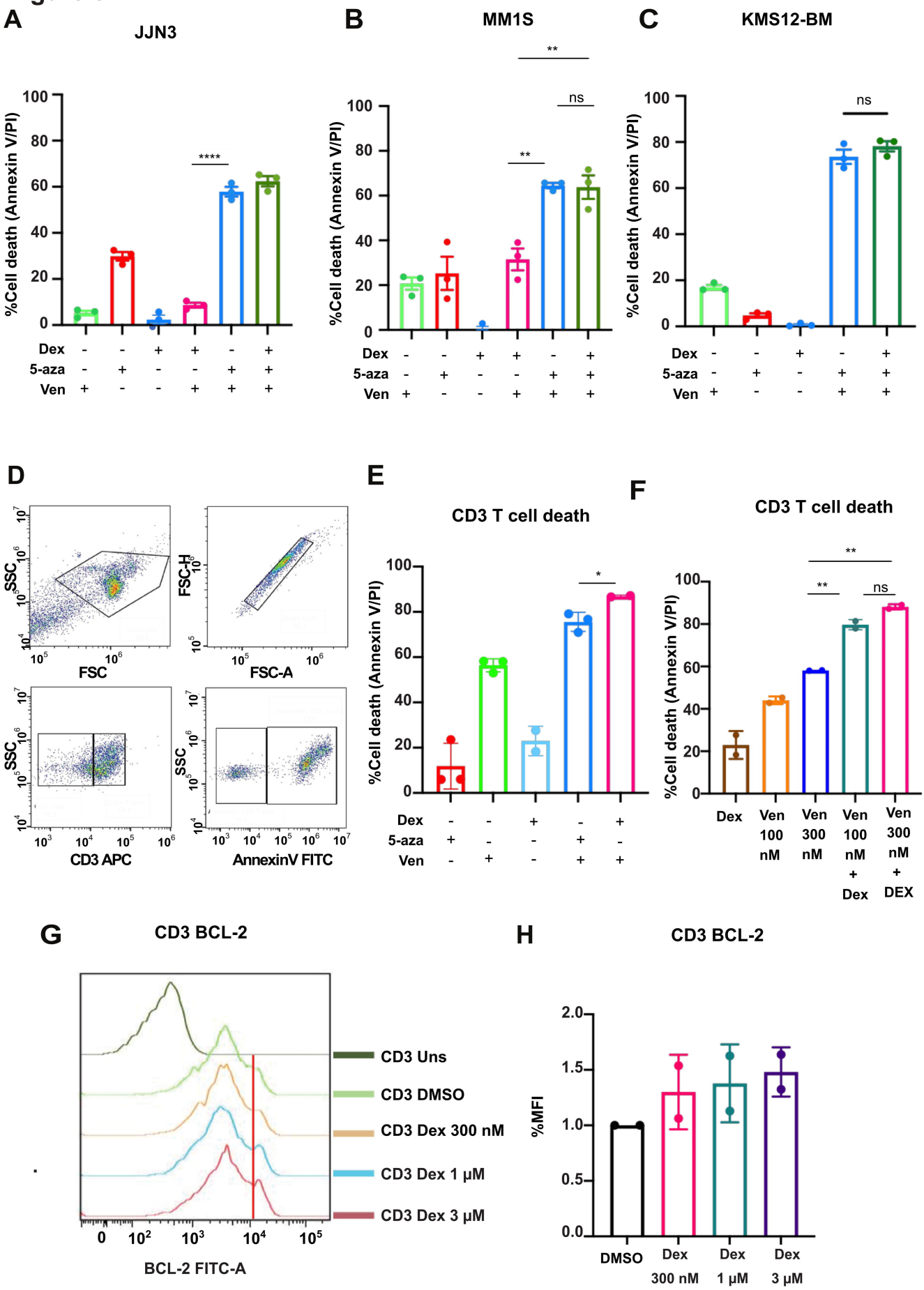
A
JJN3
%Cell death (Annexin V/PI)
****
Dex
5-aza
Ven
B
MM1S
**
ns
**
C
KMS12-BM
ns
D
SSC
FSC
FSC-H
FSC-A
CD3 APC
AnnexinV FITC
E
CD3 T cell death
*
F
CD3 T cell death
**
ns
Dex
Ven 100 nM
Ven 300 nM
Ven 100 nM + Dex
Ven 300 nM + DEX
G
CD3 BCL-2
CD3 Uns
CD3 DMSO
CD3 Dex 300 nM
CD3 Dex 1 µM
CD3 Dex 3 µM
BCL-2 FITC-A
H
CD3 BCL-2
%MFI
DMSO
Dex 300 nM
Dex 1 µM
Dex 3 µM

Figure 6

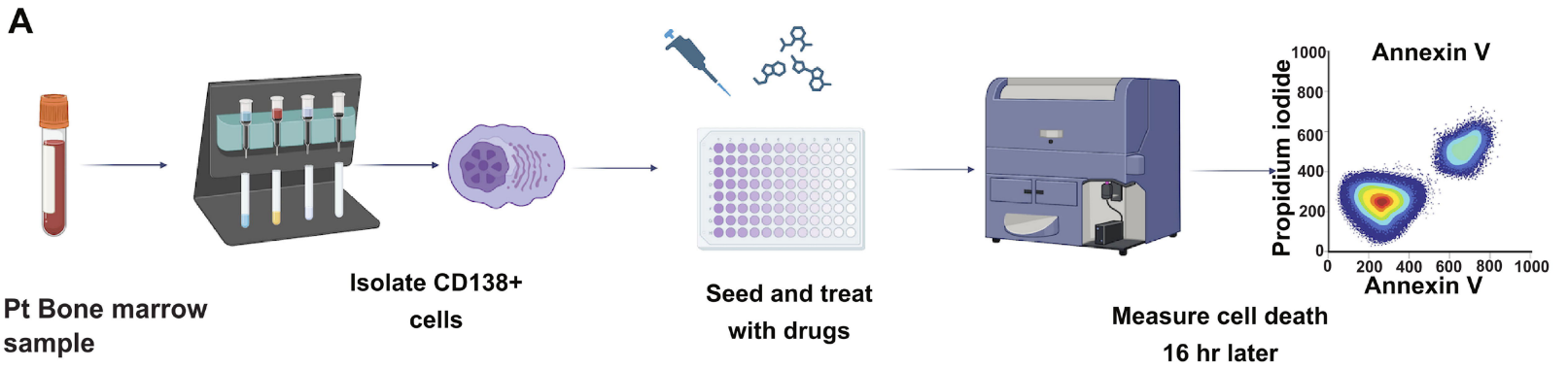
A
Pt Bone marrow sample
Isolate CD138+ cells
Seed and treat with drugs
Measure cell death 16 hr later
Annexin V
Propidium iodide
Annexin V

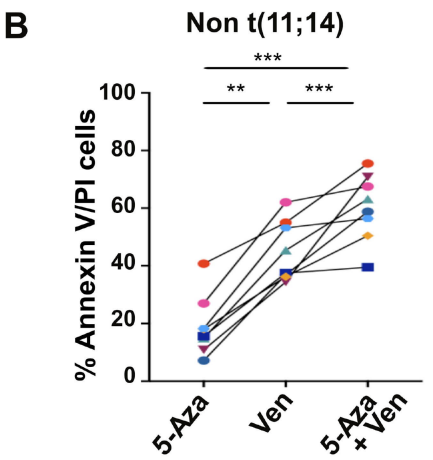
B
Non t(11;14)
% Annexin V/PI cells
5-Aza
Ven
5-Aza + Ven

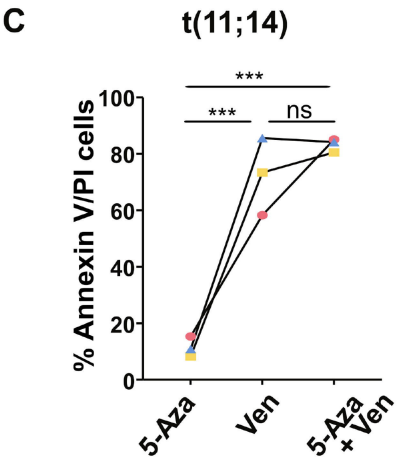
C
t(11;14)
% Annexin V/PI cells
ns
5-Aza
Ven
5-Aza + Ven

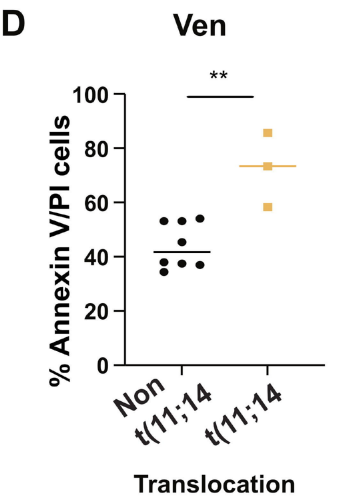
D
Ven
% Annexin V/PI cells
Non t(11;14)
t(11;14)
Translocation

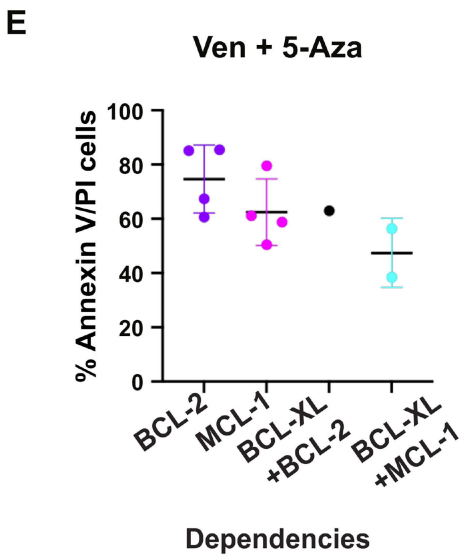
E
Ven + 5-Aza
% Annexin V/PI cells
BCL-2
MCL-1
BCL-XL +BCL-2
BCL-XL +MCL-1
Dependencies

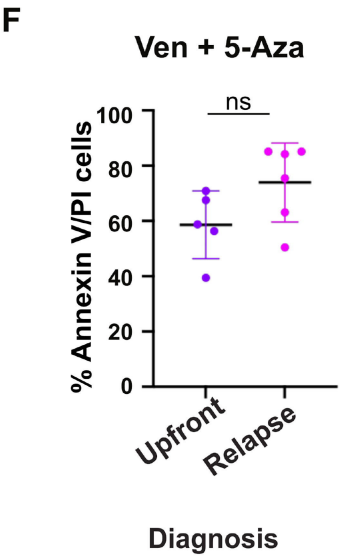
F
Ven + 5-Aza
% Annexin V/PI cells
ns
Upfront
Relapse
Diagnosis

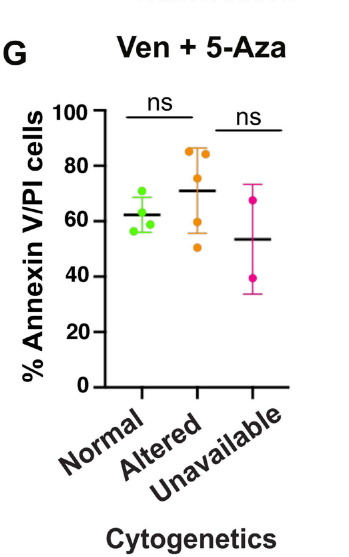
G
Ven + 5-Aza
% Annexin V/PI cells
ns
ns
Normal
Altered
Unavailable
Cytogenetics

Supplementary Materials and Methods

siRNA Transfection

JJN3 cells were counted, washed in PBS and resuspended in OptiMeM (Gibco Cat# 31985-047), 400,000 cells were combined with a mix of 4 μL Lipofectamine (Invitrogen Cat# L3000-008) and 4 μL of siRNA targeting PKR, NOXA or non-targeting control (siRNAs purchased from Dharmacon reagents, Horizon Discovery), and plated in each well a 6-well plate. RPMI 1640 medium supplemented with 10% fetal bovine serum (Gibco, Invitrogen, Carlsbad, CA, USA), 1% L-Glutamine (2 mM) (Gibco, Invitrogen, Carlsbad, CA, USA) and 1% v/v penicillin/streptomycin (50 units/ml) (Gibco, Invitrogen, Carlsbad, CA, USA) was added after 2 hours (hrs) to promote cell growth. Following 24 hrs after transfection, cells were treated with drug or DMSO control for an additional 24 hrs, then cell viability was determined using flow cytometry on the BD LSR II flow cytometer. The remaining cells were harvested for western blot analysis.

BH3 Profiling

BH3 profiling was performed using whole cell (JC-1) plate-based fluorimetry as described in the following papers(1-3). BH3 peptides (see **Table S3**) in DTEP buffer (300 mM Trehalose, 10 mM HEPES-KOH, 0.1 % w/v BSA, 1 mM EDTA, 1 mM EGTA, 80 mM KCl, 5 mM succinate, final pH 7.4) were plated at 70 μM/L (unless otherwise stated) in triplicate in a black 384-well plate. The BH3 peptides used and their binding affinities are listed in Table 1. MM cell lines were harvested, washed and resuspended in DTEP buffer. An equal volume of dye Mastermix (1 μM JC-1, 0.005% digitonin, 10 μg/ul oligomycin, 5 mM B-mercaptoethanol in DTEP buffer) was added and after 10 minutes (min) at room temperature, the cells were plated on top of the peptide

template at the concentration of 40,000 cells per well. Mitochondrial potential loss was measured using the Varioskan™ kinetic plate reader at excitation 545 nm and emission 590 nm for 3 hrs at the temperature control to 27 degrees (kinetic measurements every 5 min). Mitochondrial depolarization was normalized to DMSO control (0%) and positive control FCCP (100%) (carbonyl cyanide 4-(trifluoromethoxy) phenyl hydrazone).

Dynamic BH3 profiling

JJN3 cells were seeded at 3 x 10^6 cells in a T25 flask for 24 hrs, cells were treated with 3 μM 5-azacytidine for 20 hrs. Cells were collected, washed 1x with PBS and resuspended in 100 μL of FACS buffer (1% FBS 0.4% EDTA (2 mM) in PBS, final pH 7.4). Samples were blocked with Human Fc Block solution for 5 min (1:100) (BD Biosciences, Pharmingen, San Diego, CA cat #564219). Samples were incubated with live/dead far red stain (Invitrogen) (1:100) on ice in the dark for 30 min. Cells were pelleted at 500 x g for 5 min at 4^{o}C, washed with PBS, resuspended in DTEB buffer (300 mM Trehalose, 10 mM HEPES-KOH, 0.1% w/v BSA, 1 mM EDTA, 1 mM EGTA, 80 mM KCl, 5 mM succinate, final pH 7.4), and incubated with a panel of BH3 peptides (please see Table 1 for list of BH3 peptides and binding affinities). DTEB was added to each eppendorf tube containing twice the final concentration of each peptide treatment in 100 μL of DTEB with 0.002% w/v digitonin. The permeabilized cells were exposed to peptides for 60 min at 21 ^{o}C in the dark. Following peptide exposure, the samples were fixed with 200 μL 8% formaldehyde in PBS for 15 min at room temperature and quenched with 50 μL of 100 mM Tris / 2.5 M glycine pH 8.2 for 10 min. Cells were pelleted 1500 x g for 5 min at RT and were stained with anti-cytochrome c-FITC (#610324, Biolegend, San Diego, CA, USA) 1:100 in 0.1%

Saponin/1% BSA/PBS overnight and in dark at 4°C. The samples were resuspended in 400 μL PBS. MOMP was measured by assessing the loss of cytochrome *c* using FACS Canto II and the data was normalized to controls.

Annexin V/ Propidium Iodide staining

Apoptosis following BH3 mimetic treatment in a panel of MM cells using Annexin V-FITC/ Propidium Iodide (PI) staining. Cell lines were seeded at 3 x 10^4 cells in a 24-well plate for 24 hrs, cells were treated with venetoclax (ven), ABT-263, AMG-176, and WEHI-539 for 24 hrs. Following treatment, the cells were harvested and centrifuged at 500 g for 5 min and then washed with PBS. Each sample was re-suspended in 250 μL of Annexin V binding buffer (10 mM HEPES pH 7.4, 140 mM NaCl, 2.5 mM $CaCl_2$) Annexin V-FITC (0.25 mg/ml) and propidium iodide (PI) (1 mg/ml). Cell viability was determined using flow cytometry on the BD LSR II flow cytometer. The results were normalized to the DMSO-only control and dose-response curves were graphed using GraphPad Prism.

Western blot analysis

The cells were harvested and centrifuged at 500 rcf for 5 min. The supernatant was discarded, and the pellet was washed with PBS, before the addition of the lysis buffer. 100 μL of RIPA buffer (150 nM NaCl, 20 μM Tris, 0.5% Triton, 1 mM PMSF) was added to each sample, vortexed and incubated for 30 min on ice. The samples were then centrifuged at 12,000 RPM for 10 min. To quantify the amount of protein in each sample, the BCA assay was used, as per the manufacturer's instructions (Pierce). A total of 20 μg of protein from each sample was separated with 12% SDS-PAGE gels and transferred to nitrocellulose membranes at 40 V for 2 hrs. The blots were

incubated with the following antibodies: anti-BCL-2 (Cell Signaling Technology Cat# 15071S), anti-BCL-xL (Cell Signaling Technology Cat# 2764S), anti-MCL-1 (Cell Signaling Technology Cat# 94296), anti-NOXA (Abcam Cat# ab13654), anti-eIF2α (Cell Signaling Technology Cat# 5324S) anti-Phospho-eIF2α (Cell Signaling Technology Cat# 9721S), anti-DNMT1 (Cell Signaling Technology Cat# 5032S), anti-PKR (Invitrogen Cat#700286), anti-ATF4 (Cell Signaling Technology Cat# 11815) and anti-β-actin was used as a loading control (Sigma-Aldrich Cat# A2228). The blots were imaged using the ImageQuant LAS 4000 and analyzed using Image J software.

Immunoprecipitation

Cells were plated at 5 x 10^6 for 24 hrs and treated with DMSO or 3 μM 5-azacytidine for 24 hrs. Cellular proteins were extracted and cell lysates (500 μg) were pre-cleared with 20 μl of agarose beads (Piece Protein A Agarose, Thermofisher cat no. 20333) and rotated for 1 hr at 4°C at 3 RPM. Cell lysates (500 μg) were then subjected to immunoprecipitation by incubating with 40 μl of agarose beads and 20 μl of MCL-1 antibody (Cell Signaling Technology Cat# 94296) or IgG control in the presence of protease inhibitors overnight at 4°C rotating at 3 RPM. The immunocomplexes were applied to 18% SDS-polyacrylamide gels and blotted to a nitrocellulose membrane for Western blotting.

Co-culture with fibroblasts

JJN3, MM1S, HS-5 and MM-BMSC were cultured in RPMI 1640 medium supplemented with 10% fetal bovine serum (Gibco, Invitrogen, Carlsbad, CA, USA), 1% L-Glutamine (2 mM) (Gibco, Invitrogen, Carlsbad, CA, USA) and 1% v/v penicillin/streptomycin (50 units/ml) (Gibco, Invitrogen, Carlsbad, CA, USA). For the

co-culture system, HS-5 or MM-BMSC cells were seeded in a 24-well plate at 5 x 10^4 cells for 24 hrs. The day after 1 x 10^5 JJN3 or MM1S cells were seeded on top of the confluent monolayer for 24 hrs. Cells were treated with 5-azacytidine (5-aza), ven or 5-aza and ven for 24 hrs and cell viability was assessed using Annexin V/PI staining.

CD138$^+$ cell isolation from primary MM bone marrow samples

Ethical approval was granted from the Beaumont hospital and RCSI ethics committee, study number 19/32. Upon receipt of a primary patient sample, red cell lysis buffer (Roche) is added at 3 times the volume of the patient sample and incubated at room temperature for 10 min. The sample is then centrifuged at 1500 rpm for 5 min and the supernatant is discarded. The pellet is resuspended in 20 mL PBS for the total cell count. The sample is centrifuged again and resuspended in the appropriate amount of CD138 magnetic beads and MACS buffer (Miltenyi Biotec) 20 μL of beads per 10 million cells, 80 μL of buffer per 10 million cells. The sample is incubated on ice for 15 min before 20 mL of MACS buffer is added and the sample is centrifuged. The supernatant is removed, and the sample is resuspended in 1 mL of MACS buffer. The sample is run through the magnetic LS column, followed by 3 x 3 mL washes with MACS buffer. The CD138$^+$ cells are collected and counted. Once counted, CD138$^+$ cells were seeded at 1 x 10^4 cells per well in a 96-well plate. Cells were treated with BH3 mimetics (ABT-199, A-1331852, AMG-176) at doses ranging from 30 nM to 3 μM, 5-aza 3 μM +/- ven 100 nM or 300 nM, for 16 hrs. Cell viability was assessed using Annexin V/PI staining as described above. The MM-BMSC cells were grown by harvesting the negative fraction of cells that ran through the CD138$^+$ column. The cells were washed with PBS then seeded into a T25 with RPMI media and grown for two

weeks until a confluent layer of fibroblasts was cultured. The MM-BMSC cells were then seeded for further experiments.

Epigenetic modifier screen using CellTiter-Glo®

Cells were seeded in a 96-well plate at a density of 1 x 10^4 cells per well for 24 hrs and treated with 2 doses (500 nM, 100 nM) of epigenetic modifier (see Table S1) alone and in combination with ven (1 μM for 24 hrs). Following treatment, 20 μL of CellTiter-Glo® is added to each well at RT for 30 min. Luminescence is read on the ClarioStar plate reader as per the manufacturer's instructions. The results were normalized to the DMSO-only control and heatmaps were graphed using Graphpad Prism.

Live cell microscopy

JJN3 cells were seeded at 15,000 cells/well in a μ-Slide 8-well high chambers (Ibidi, cat no. 80801) for 24 hrs and treated with DMSO, 5-azacytidine 3 μM, ven 1 μM and 5-azacytidine and ven for 24 hrs. PKMO(4) (Spirochrome, cat no. SC053) and Picogreen staining (0.1%) (Thermofisher, cat no. P11495) was added at 300 nM concentration for 20 min in RPMI 1640 cell culture medium at 37°C. Cells were washed twice with warmed medium and imaged via confocal microscopy on a Leica Stellaris 8 system. A minimum of 5 images were taken for each condition and analysed using Fiji software.

dsRNA staining

For immunofluorescence microscopy, JJN3 cells were seeded at 3 x 10^4 cells in a 24-well plate for 24 hrs. Following this, the cells were treated with DMSO, 5-azacytidine 3 μM, ven 1 μM or 5-azacytidine and ven for 24 hrs. The cells were harvested and

washed in PBS. The cells were incubated with 200 nM mitotracker red (Invitrogen, cat no. M22425) for 30 min protected from light at 37°C. The cells were washed twice with PBS and cytospun at 400 x rcf for 6 minutes onto glass slides. The cells were fixed with ice-cold 4% paraformaldehyde (PFA) for 15 min protected from light. The cells were washed 3 times with ice-cold PBS and permeabilized with Triton-X100 (0.5%) for 15 minutes. The cells were washed 3 times with PBS and blocked with 5% BSA/Hoechst (1:1000) for 1 hr. The cells were washed in PBS before being incubated with anti-dsRNA (1:700) overnight at 4°C (Sigma-Aldrich, cat no. MABE1134). The cells with incubated for 2 hrs in secondary antibody (Goat anti-mouse IgM, Alexa Fluor 594, Invitrogen, cat no. A-21044) diluted in 5% BSA at room temperature. After washing the cells with PBS, the coverslip was mounted to the glass slide using mounting medium and allowed to dry at room temperature for a 2 hrs. The slides were imaged via confocal microscopy on a Leica Stellaris 8 system. 5 images were taken per treatment and images were analysed using Fiji software.

Peripheral Blood Mononuclear Cells (PBMC) Annexin V/Propidium Iodide staining

Apoptosis following treatment with 5-azacytidine/ven and bortezomib, dexamethasone and ven in PBMCs using AnnexinV-FITC/ Propidium Iodide (PI) staining. PBMCs were seeded at 3 x 10^4 cells in a 96-well plate, cells were treated with 5-azacytidine alone, ven alone or in combination for 16 hrs. Additionally, cells were treated with bortezomib alone, dexamethasone alone, ven alone or in combination for 16 hrs. Following treatment, the cells were stained with cell surface markers CD19 (Miltenyi; cat no. 561295) and CD3 (Miltenyi; cat no. 317317) for 30 min on ice protected from light. The cells were then centrifuged at 500 g for 5 min and then washed with PBS. Each sample was assessed for Annexin V/Pi staining as described previously. Cell viability was

determined using flow cytometry on the BD LSR II flow cytometer. The results were normalized to the DMSO-only control and dose-response curves were graphed using GraphPad Prism.

Intracellular BCL-2 staining

PBMCs were seeded at 1 x 10^5 cells in a 96-well plate and treated with increasing concentrations of dexamethasone for 16 hrs. PBMCs were harvested and resuspended in 100 uL of 1% BSA/PBS and blocked with a human FcR blocker (1:100) for 10 min on ice. Cells were then stained with anti-CD3-APC (cat no. 555335) at 1:100 dilutions for 30 min on ice protected from light. Cells were fixed in 2% formaldehyde for 15 min protected from light and neutralized with 1M Tris for 5 min. Cells were resuspended in staining buffer (1% BSA, 2% FBS, 0.1% Saponin and 1.5 mM NaN3 in PBS) and stained with BCL-2 FITC (cat no. 130-114-339) and IgG control overnight at 4 ^{o}C. Following washing, the cells were resuspended in PBS and BCL-2 protein expression was determined using flow cytometry on the BD LSR II flow cytometer.

Data and statistical analyses

GraphPad Prism 9.0 software was used for all statistical analyses. Dose-response curves and IC_{50} values were calculated using linear regression curve fit (Log inhibitor vs. normalized response, variable slope). Unless otherwise stated, the results are expressed as the mean $\pm$ standard error of the mean (SEM) of three independent experiments.

Supplementary Figure Legends

Figure S1. BH3 profiling and BH3 mimetics identify diverse anti-apoptotic dependence in MM cell lines.

A) The induction of cell death by BH3 mimetics ABT-199, ABT-263, WEHI-529 and AMG-176 in the JJN3 cells was measured by annexin V/PI. Graphed in the dose-response curves are the mean +/- SEM of three biological repeats. The IC_{50} values are listed below the graph. B) similar to A) for the KMS18 cell line. C) Cell viability following treatment with BH3 mimetics (left) and BH3 profile (right) for C) MM1S D) KMS12-BM E) KMS-27 F) H929 G) RPMI-8266 H) U266 cells. Cells were treated with increasing doses of ABT-199, ABT-263, WEHI-539 or A-1331852 and AMG-176 for 24 hrs and cell viability was assessed by annexin V/PI staining. Cells were treated with a series of BH3 peptides at the listed concentrations. The mitochondrial membrane potential was measured using JC-1. Graphed is the normalized mitochondrial potential (based on positive and negative controls) mean ± SEM of three independent experiments.

Figure S2. Assessing potential hits from the initial epigenetic screen in JJN3 MCL-1 dependent cells.

Cell viability was assessed in JJN3 cells using annexin V/PI staining following 24 hr treatment with or without the following epigenetic modifiers A) JIB-04, B) GSK-J4 C) Panobinostat D) 5-aza E) Belinostat F) Curcumin G) CPI023 H) Decitabine I) BAS-2 J) Citarinostat K) UNC-1215 L) I-BET151 +/- 1 μM ven. Graphed are the mean values ± SEM from three independent experiments. The green dot shows the viability of 1 μM ven.

Figure S3. Assessing potential hits from the initial epigenetic screen in KMS-18 a BCL-2/BCL-xL dependent cells.

Cell viability was assessed in KMS18 cells using annexin V/PI staining following 24 hr treatment with the following epigenetic modifiers A) JIB-04, B) Panobinostat C) 5-aza D) GSK-J4 E) Citarinostat F) Belinostat G) BAS-2 H) Curcumin I) Decitabine J) UNC-1215 K) CPI-023 L) I-BET151 +/- 500 nM ven. Graphed are the mean values ± SEM from three independent experiments. The green dot shows the viability of 500 nM ven.

Figure S4. Validating the combination of ven and 5-aza in a panel of MM cell lines.

Cell viability was assessed in A) MM1S) B) H929 C) KMS-27 D) KMS-18 E) KMS12-BM cells using annexin V/PI staining following 24-hour treatment with listed doses of ven with or without 3 μM 5-aza. Graphed are the mean values ± SEM from three independent experiments, and the IC_{50} values are listed on the graph. F) Based on the dose-response curves shown in A-E the area under the curve of ven alone or ven + 5-aza 3 μM was calculated and the ratio was graphed. G) The combination index was calculated for a series of ven doses with 5-aza 3 μM using Webb's fractional product and is visualized by a heatmap with the combination index listed for each treatment. H) The combination index for KMS-27 was graphed in a heatmap separately due to the lower dose of ven. Cell viability was assessed in I) MM1S) J) KMS-189 K) RPMI-8266 L) JJN3 M) U266 cells using annexin V/PI staining following 24-hour treatment with listed doses of 5-aza with or without 1 μM ven (500 nM ven for KMS-18). N) the ratio of the area under the curve of each dose-response curve is

graphed O) The combination index of different doses of 5-aza with 1 μM ven (500 nM ven for KMS-18) is represented by a heatmap.

Figure S5. Molecular analysis of 5-azacytidine treatment in cells.

(A) Western blot analysis of DNMT1 expression following a dose-response with 5-azacytidine treatment at 24 hr. Actin blot demonstrates loading control. B) Densitometry of BIM and NOXA bound to MCL-1 following DMSO or 5-AZA 3 μM treatment. C) Densitometry of PKR siRNA Western blots shown in Figure 3H, where the data was normalized to actin densitometry. The densitometry was then normalized to each treatment to show that a downregulation by the siRNA (A mean of two independent Western blots are graphed). D) Densitometry of NOXA siRNA Western blots shown in Figure 3I, where the data was normalized to actin densitometry. The densitometry was then normalized to each treatment to show that a downregulation by the siRNA (A mean of two independent Western blots are graphed).

Figure S6. Ven and 5-azacytidine combination enhances cell death in primary MM samples *ex-vivo.* A-K) Individual graphs of cell viability following 16 hr treatment with (left) BH3 mimetics or (right) 5-azacytidine, ven and in combination. Error bars indicate duplicate measurements. L) Protein expression analysis of primary samples and MM cell lines.

Figure S7. Non-normalized ven and 5-azacytidine combination in primary MM samples *ex-vivo.* A-K) Individual graphs of cell viability following 16 hr treatment with (left) BH3 mimetics or (right) 5-azacytidine, ven and in combination. Error bars indicate duplicate measurements.

Patient number	Date of recruitment	M/F	Age	Cytogenetics	No. of prior treatments	Stage of MM
1	13/01/2022	M	60	Normal cytogenetics	NDMM, no previous treatment	ISS 2
2	26/07/2022	F	55	Cytogenetics unavailable	NDMM, no previous treatment	Data unavailable
3	19/05/2021	M	55	Normal cytogenetics	NDMM, no previous treatment	ISS 2
4	23/09/2021	M	58	P53 deletion	Five prior lines – CVD, R, IRD, DPD, KD	ISS 3
5	05/05/2021	F	78	Normal cytogenetics	First relapse – previous CVD	ISS 2
6	14/02/2022	M	59	1q amplification	Six prior lines – RVD, CVD, KD, PD, DVD, CPD-Dara clinical trial, IxaDex	ISS 3
7	20/04/2021	M	91	Cytogenetics available	NDMM, no previous treatment	Data unavailable
8	03/03/2022	M	54	Normal cytogenetics	NDMM, no previous treatment	ISS 2
9	02/09/2021	F	58	P53 deletion, t(11;14) translocation	Five prior lines – RVD, KD, DPD, IRD, PD	ISS 2
10	10/03/2021	M	69	P53 deletion, loss of CDKN2C/CKS18, t(11;14) translocation	Two prior lines – CVD, KRD	ISS 3
11	28/10/2021	F	76	IGH/CCN1 rearrangement, t(11;14) translocation	First relapse – previous RVD	ISS 2

Table S1. Patient clinical database.

Listed in the table are the characteristics including, sex, age, cytogenetics, staging and prior treatments for each of the patients who generously provided a sample for analysis.

References

1. Ni Chonghaile T, Sarosiek KA, Vo TT, et al. Pretreatment mitochondrial priming correlates with clinical response to cytotoxic chemotherapy. Science. 2011 Nov 25;334(6059):1129-33. eng. Epub 20111027. doi:10.1126/science.1206727. Cited in: Pubmed; PMID 22033517.
2. Chonghaile TN, Roderick JE, Glenfield C, et al. Maturation stage of T-cell acute lymphoblastic leukemia determines BCL-2 versus BCL-XL dependence and sensitivity to ABT-199. Cancer Discov. 2014 Sep;4(9):1074-87. Epub 2014/07/06. doi:10.1158/2159-8290.CD-14-0353. Cited in: Pubmed; PMID 24994123.
3. Touzeau C, Ryan J, Guerriero J, et al. BH3 profiling identifies heterogeneous dependency on Bcl-2 family members in multiple myeloma and predicts sensitivity to BH3 mimetics. Leukemia. 2016 Mar;30(3):761-4. Epub 2015/07/16. doi:10.1038/leu.2015.184. Cited in: Pubmed; PMID 26174630.
4. Liu T, Stephan T, Chen P, et al. Multi-color live-cell STED nanoscopy of mitochondria with a gentle inner membrane stain. Proc Natl Acad Sci U S A. 2022 Dec 27;119(52):e2215799119. Epub 2022/12/20. doi:10.1073/pnas.2215799119. Cited in: Pubmed; PMID 36534799.

Figure S1

A

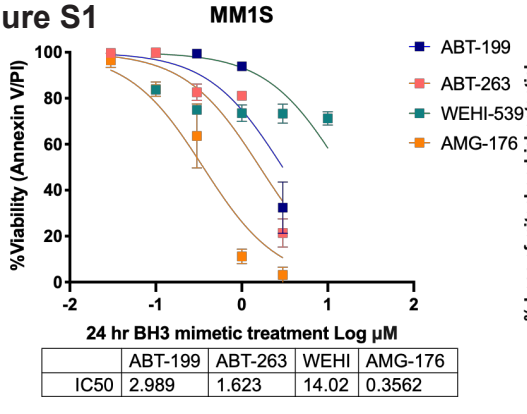

	ABT-199	ABT-263	WEHI	AMG-176
IC50	2.989	1.623	14.02	0.3562

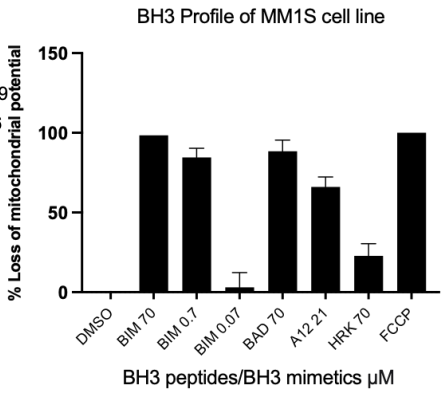

B

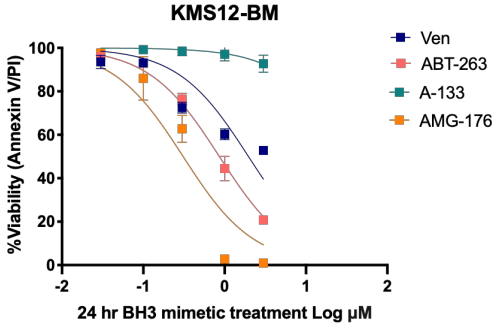

	ABT-199	ABT-263	A-133	AMG-176
IC50	1.963	0.8612	37.21	0.3086

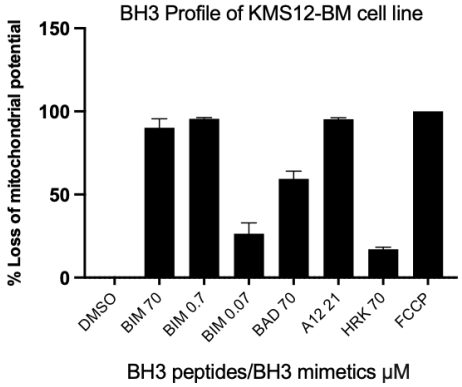

C

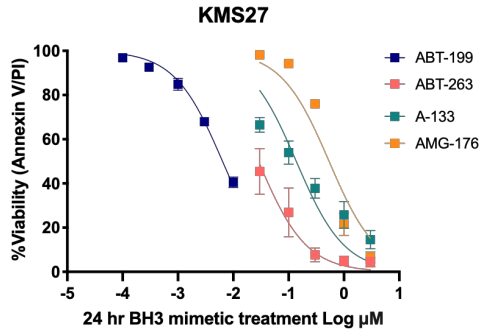

	ABT-199	ABT-263	AMG-176	A-133
IC50	0.006395	0.02848	0.5388	0.1376

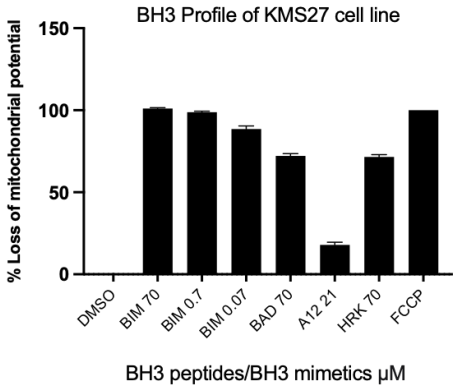

D

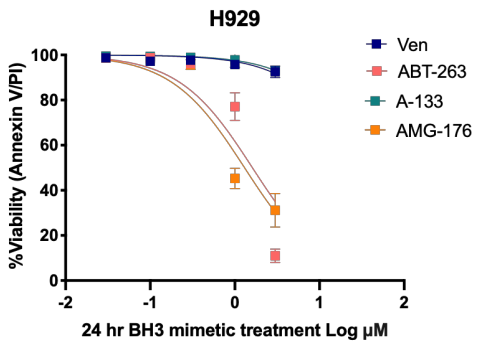

	ABT-199	ABT-263	A-133	AMG-176
IC50	33.23	1.613	40.58	1.303

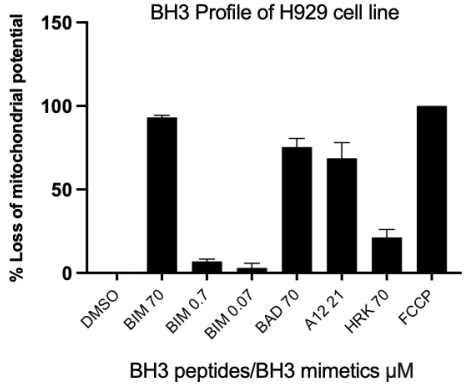

E

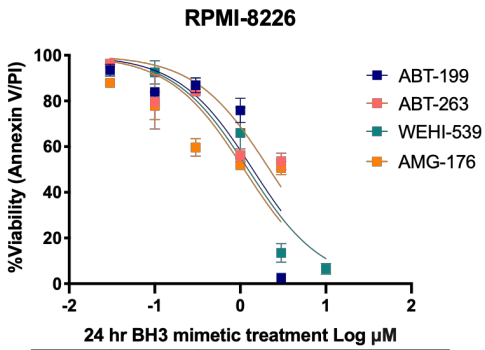

	ABT-199	ABT-263	WEHI	AMG-176
IC50	1.401	2.198	1.235	1.109

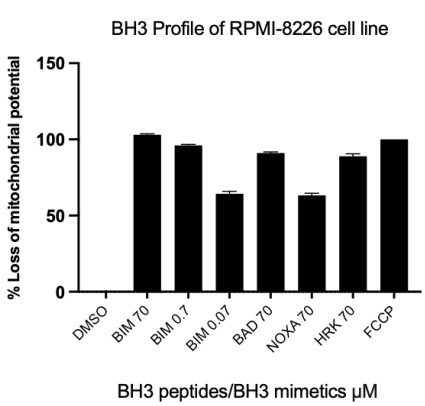

F

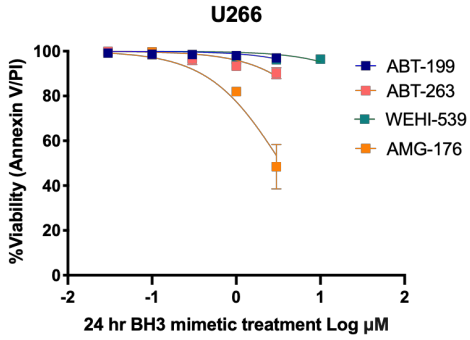

	ABT-199	ABT-263	WEHI	AMG-176
IC50	84.28	23.85	201.2	3.442

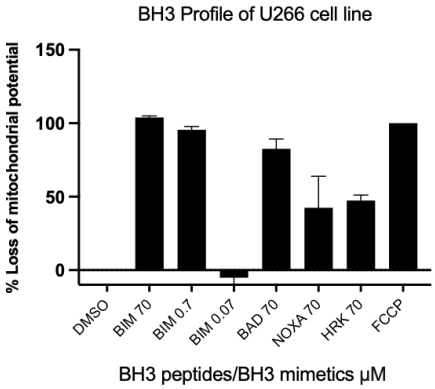

H

Figure S2

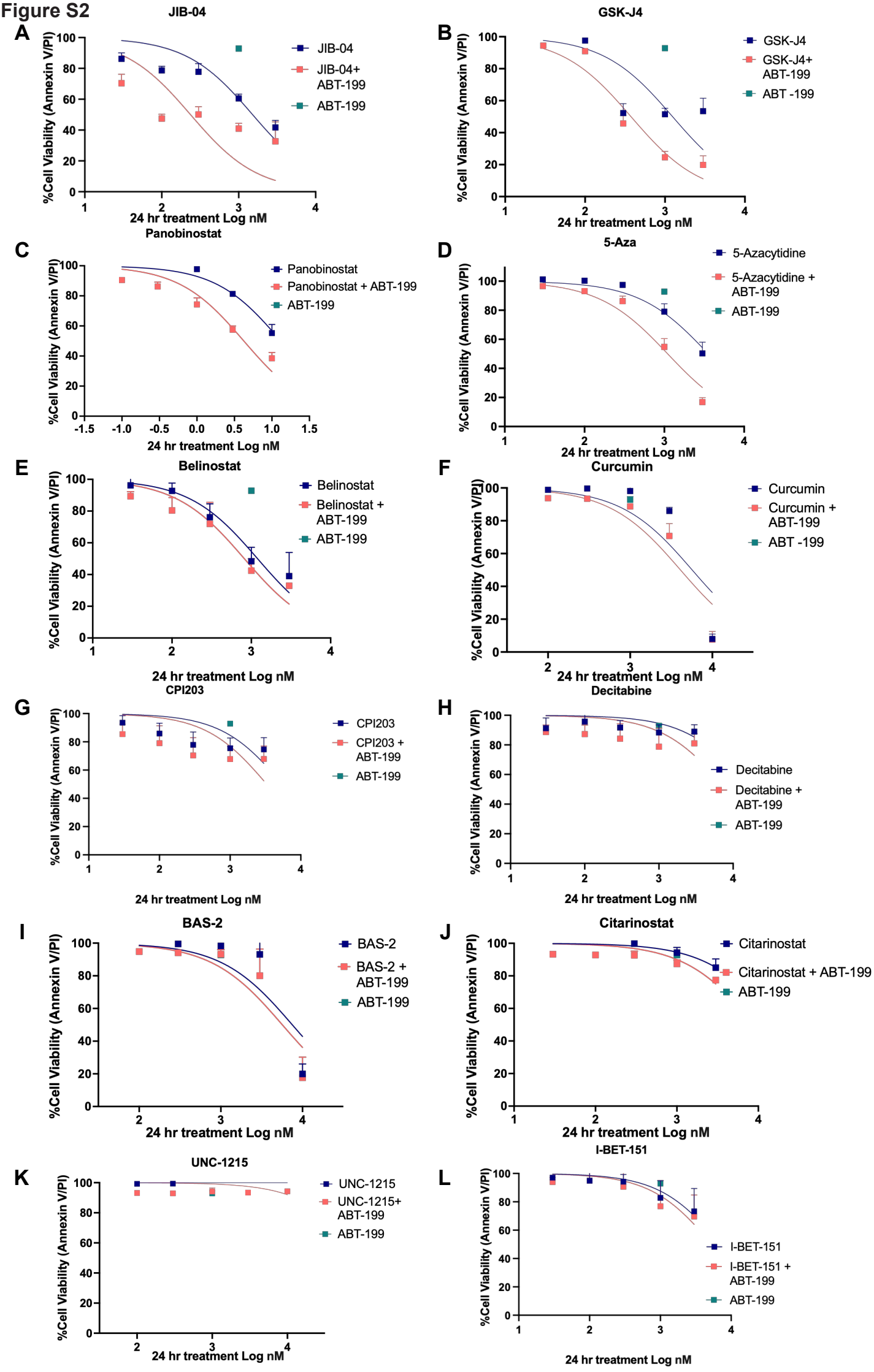
A
JIB-04
%Cell Viability (Annexin V/PI)
24 hr treatment Log nM
JIB-04
JIB-04+ ABT-199
ABT-199
B
GSK-J4
GSK-J4
GSK-J4+ ABT-199
ABT -199
C
Panobinostat
Panobinostat
Panobinostat + ABT-199
ABT-199
D
5-Aza
5-Azacytidine
5-Azacytidine + ABT-199
ABT-199
E
Belinostat
Belinostat
Belinostat + ABT-199
ABT-199
F
Curcumin
Curcumin
Curcumin + ABT-199
ABT -199
G
CPI203
CPI203
CPI203 + ABT-199
ABT-199
H
Decitabine
Decitabine
Decitabine + ABT-199
ABT-199
I
BAS-2
BAS-2
BAS-2 + ABT-199
ABT-199
J
Citarinostat
Citarinostat
Citarinostat + ABT-199
ABT-199
K
UNC-1215
UNC-1215
UNC-1215+ ABT-199
ABT-199
L
I-BET-151
I-BET-151
I-BET-151 + ABT-199
ABT-199

Figure S3

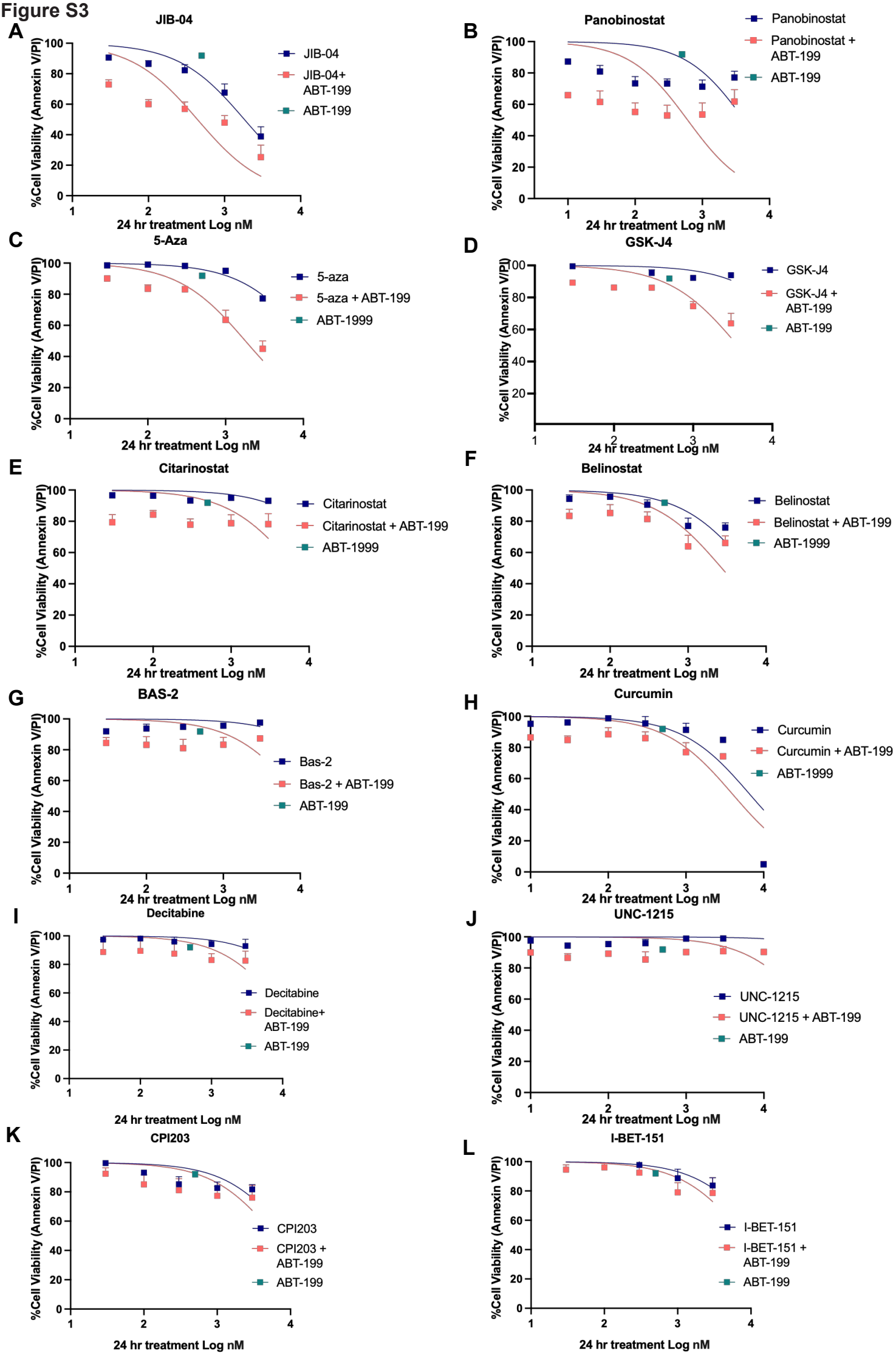
A
JIB-04
%Cell Viability (Annexin V/PI)
24 hr treatment Log nM
JIB-04
JIB-04+ ABT-199
ABT-199
B
Panobinostat
Panobinostat
Panobinostat + ABT-199
ABT-199
C
5-Aza
5-aza
5-aza + ABT-199
ABT-1999
D
GSK-J4
GSK-J4
GSK-J4 + ABT-199
ABT-199
E
Citarinostat
Citarinostat
Citarinostat + ABT-199
ABT-1999
F
Belinostat
Belinostat
Belinostat + ABT-199
ABT-1999
G
BAS-2
Bas-2
Bas-2 + ABT-199
ABT-199
H
Curcumin
Curcumin
Curcumin + ABT-199
ABT-1999
I
Decitabine
Decitabine
Decitabine+ ABT-199
ABT-199
J
UNC-1215
UNC-1215
UNC-1215 + ABT-199
ABT-199
K
CPI203
CPI203
CPI203 + ABT-199
ABT-199
L
I-BET-151
I-BET-151
I-BET-151 + ABT-199
ABT-199

Figure S4

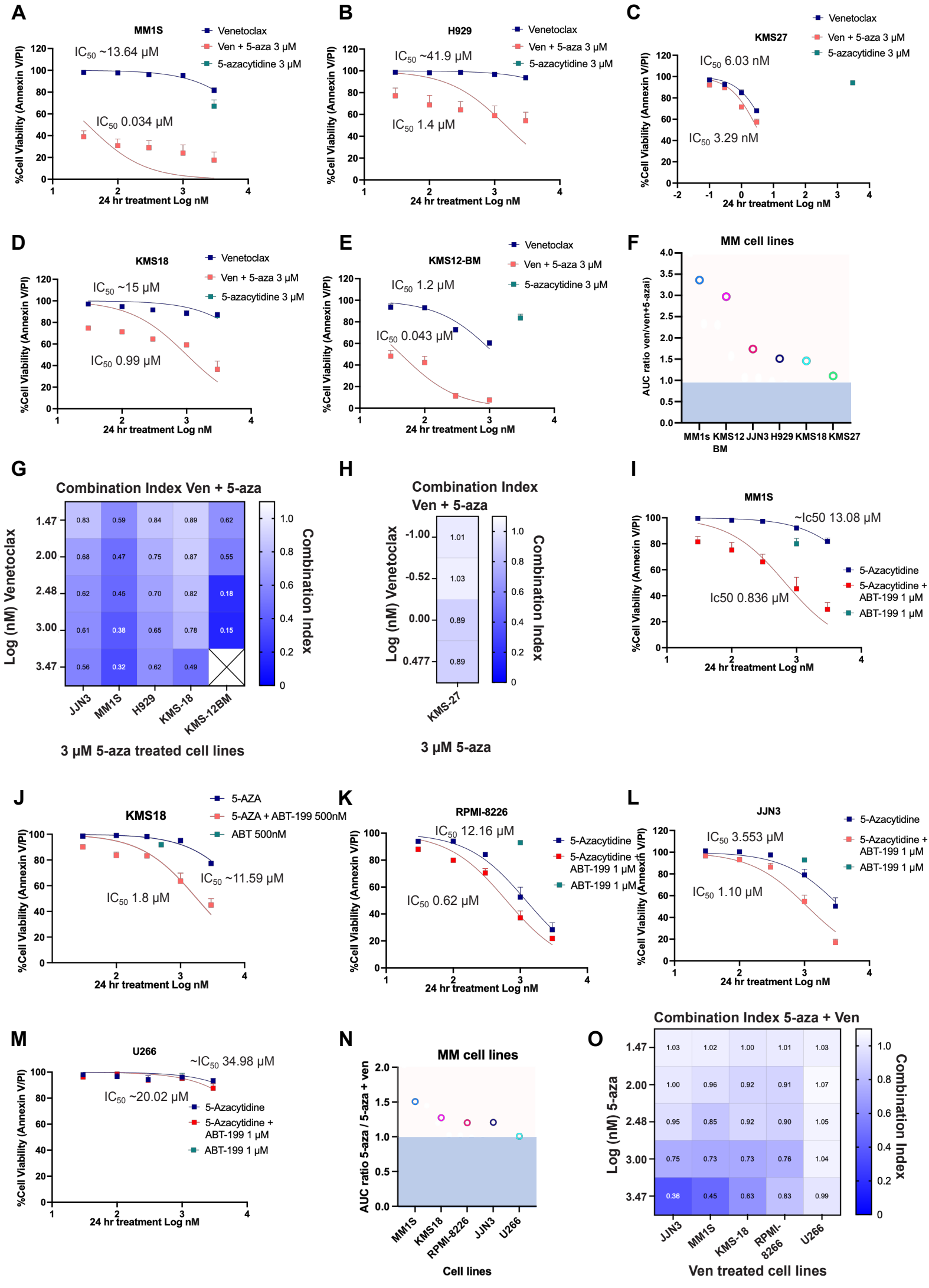
A
MM1S
Venetoclax
Ven + 5-aza 3 μM
5-azacytidine 3 μM
IC50 ~13.64 μM
IC50 0.034 μM
%Cell Viability (Annexin V/PI)
24 hr treatment Log nM
B
H929
IC50 ~41.9 μM
IC50 1.4 μM
C
KMS27
IC50 6.03 nM
IC50 3.29 nM
D
KMS18
IC50 ~15 μM
IC50 0.99 μM
E
KMS12-BM
IC50 1.2 μM
IC50 0.043 μM
F
MM cell lines
AUC ratio ven/ven+5-azai
MM1s
KMS12 BM
JJN3
H929
KMS18
KMS27
G
Combination Index Ven + 5-aza
Log (nM) Venetoclax
1.47
2.00
2.48
3.00
3.47
0.83 0.59 0.84 0.89 0.62
0.68 0.47 0.75 0.87 0.55
0.62 0.45 0.70 0.82 0.18
0.61 0.38 0.65 0.78 0.15
0.56 0.32 0.62 0.49
JJN3
MM1S
H929
KMS-18
KMS-12BM
Combination Index
3 μM 5-aza treated cell lines
H
Combination Index
Ven + 5-aza
-1.00
-0.52
0.00
0.477
1.01
1.03
0.89
0.89
KMS-27
3 μM 5-aza
I
MM1S
~Ic50 13.08 μM
Ic50 0.836 μM
5-Azacytidine
5-Azacytidine + ABT-199 1 μM
ABT-199 1 μM
J
KMS18
5-AZA
5-AZA + ABT-199 500nM
ABT 500nM
IC50 ~11.59 μM
IC50 1.8 μM
K
RPMI-8226
IC50 12.16 μM
IC50 0.62 μM
L
JJN3
IC50 3.553 μM
IC50 1.10 μM
M
U266
~IC50 34.98 μM
IC50 ~20.02 μM
N
MM cell lines
AUC ratio 5-aza / 5-aza + ven
MM1S
KMS18
RPMI-8226
JJN3
U266
Cell lines
O
Combination Index 5-aza + Ven
Log (nM) 5-aza
1.47
2.00
2.48
3.00
3.47
1.03 1.02 1.00 1.01 1.03
1.00 0.96 0.92 0.91 1.07
0.95 0.85 0.92 0.90 1.05
0.75 0.73 0.73 0.76 1.04
0.36 0.45 0.63 0.83 0.99
JJN3
MM1S
KMS-18
RPMI-8266
U266
Ven treated cell lines

Figure S5

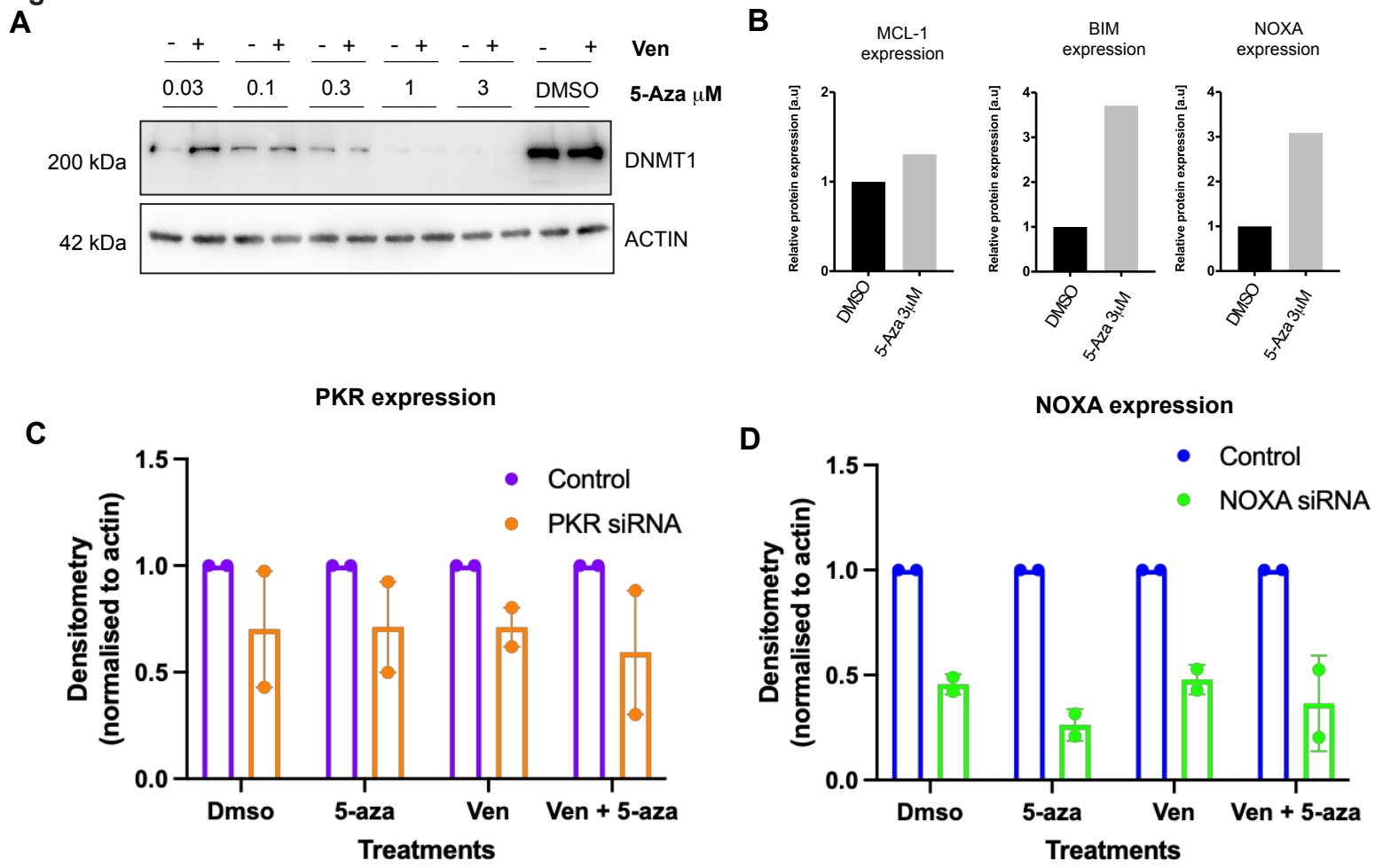
A
- + - + - + - + - + - + Ven
0.03 0.1 0.3 1 3 DMSO 5-Aza μM
200 kDa
DNMT1
42 kDa
ACTIN
B
MCL-1 expression
BIM expression
NOXA expression
Relative protein expression [a.u]
DMSO
5-Aza 3μM

C
PKR expression
Control
PKR siRNA
Densitometry (normalised to actin)
Dmso
5-aza
Ven
Ven + 5-aza
Treatments

D
NOXA expression
Control
NOXA siRNA
Densitometry (normalised to actin)
Dmso
5-aza
Ven
Ven + 5-aza
Treatments

Figure S6

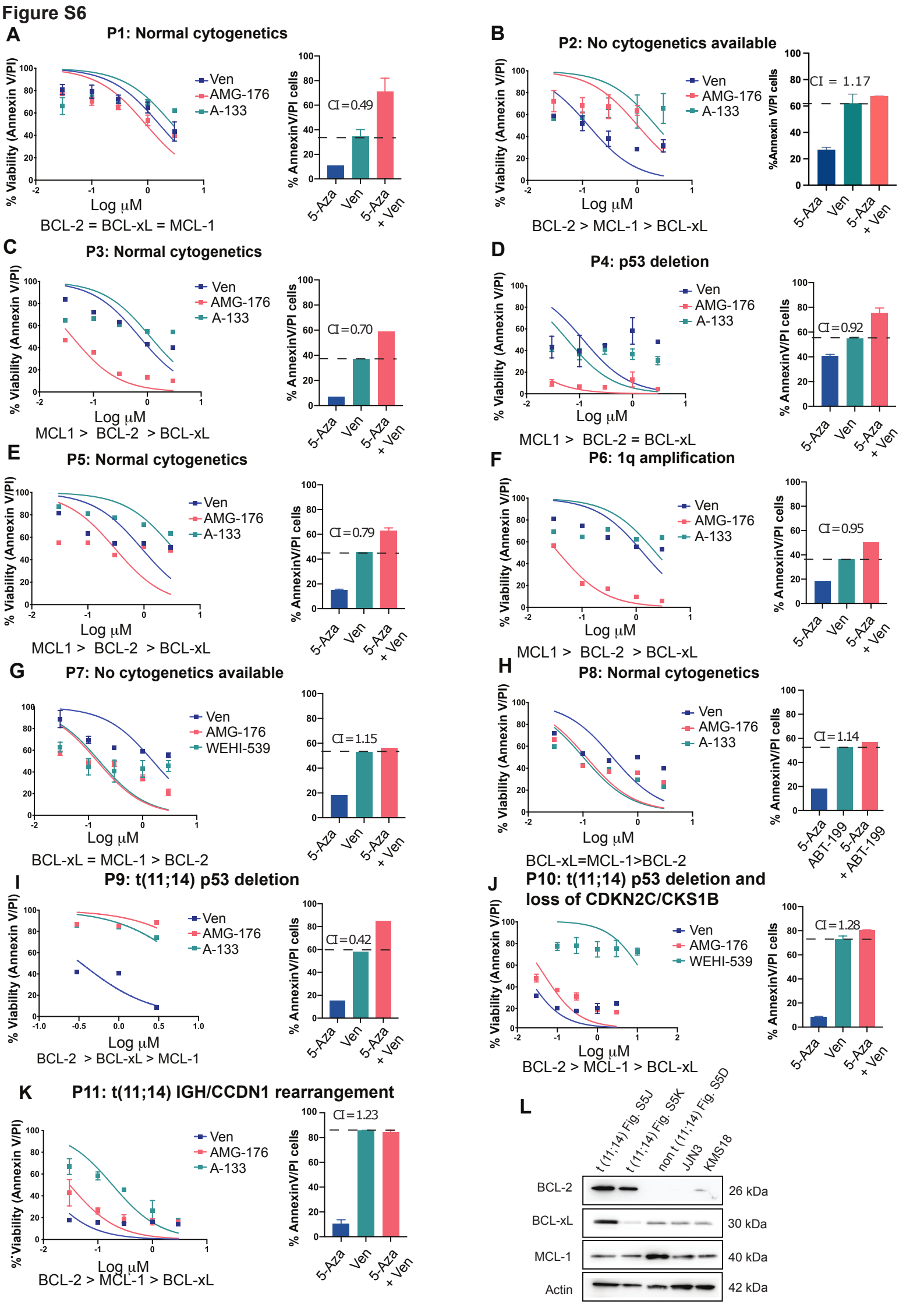
A
P1: Normal cytogenetics
% Viability (Annexin V/PI)
Log μM
Ven
AMG-176
A-133
BCL-2 = BCL-xL = MCL-1
% AnnexinV/PI cells
CI=0.49
5-Aza
Ven
5-Aza + Ven
B
P2: No cytogenetics available
BCL-2 > MCL-1 > BCL-xL
CI = 1.17
C
P3: Normal cytogenetics
MCL1 > BCL-2 > BCL-xL
CI=0.70
D
P4: p53 deletion
MCL1 > BCL-2 = BCL-xL
CI=0.92
E
P5: Normal cytogenetics
MCL1 > BCL-2 > BCL-xL
CI=0.79
F
P6: 1q amplification
MCL1 > BCL-2 > BCL-xL
CI=0.95
G
P7: No cytogenetics available
WEHI-539
BCL-xL = MCL-1 > BCL-2
CI=1.15
H
P8: Normal cytogenetics
BCL-xL=MCL-1>BCL-2
CI=1.14
5-Aza
ABT-199
5-Aza + ABT-199
I
P9: t(11;14) p53 deletion
BCL-2 > BCL-xL > MCL-1
CI=0.42
J
P10: t(11;14) p53 deletion and loss of CDKN2C/CKS1B
BCL-2 > MCL-1 > BCL-xL
CI=1.28
K
P11: t(11;14) IGH/CCDN1 rearrangement
BCL-2 > MCL-1 > BCL-xL
CI=1.23
L
t (11;14) Fig. S5J
t (11;14) Fig. S5K
non t (11;14) Fig. S5D
JJN3
KMS18
BCL-2
BCL-xL
MCL-1
Actin
26 kDa
30 kDa
40 kDa
42 kDa

Figure S7

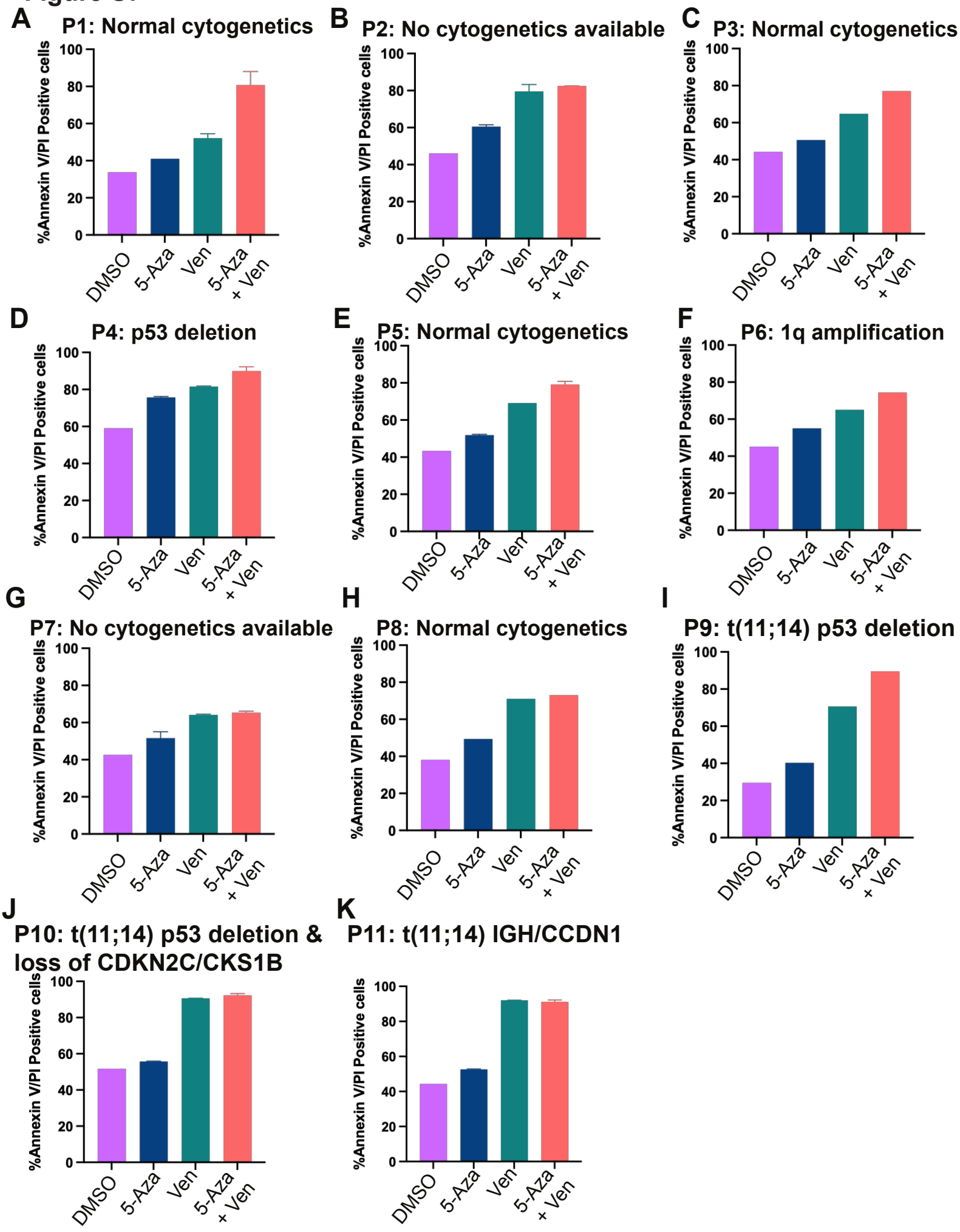
A
P1: Normal cytogenetics
B
P2: No cytogenetics available
C
P3: Normal cytogenetics
D
P4: p53 deletion
E
P5: Normal cytogenetics
F
P6: 1q amplification
G
P7: No cytogenetics available
H
P8: Normal cytogenetics
I
P9: t(11;14) p53 deletion
J
P10: t(11;14) p53 deletion & loss of CDKN2C/CKS1B
K
P11: t(11;14) IGH/CCDN1
%Annexin V/PI Positive cells
0
20
40
60
80
100
DMSO
5-Aza
Ven
5-Aza + Ven